# Quantification of the hadronic and leptonic gamma-ray components in the TeV gamma ray supernova remnant RX J1713.7−3946

Yasuo Fukui
Nagoya U.

Collaborators : Hidetoshi Sano2,
Yumiko Yamane1, Takahiro Hayakawa1,
Tsuyoshi Inoue1, Gavin Rowell3,
and Sabrina Einecke3

1 Nagoya U.
2 National Astronomical Obs.
3 Adelaide U.

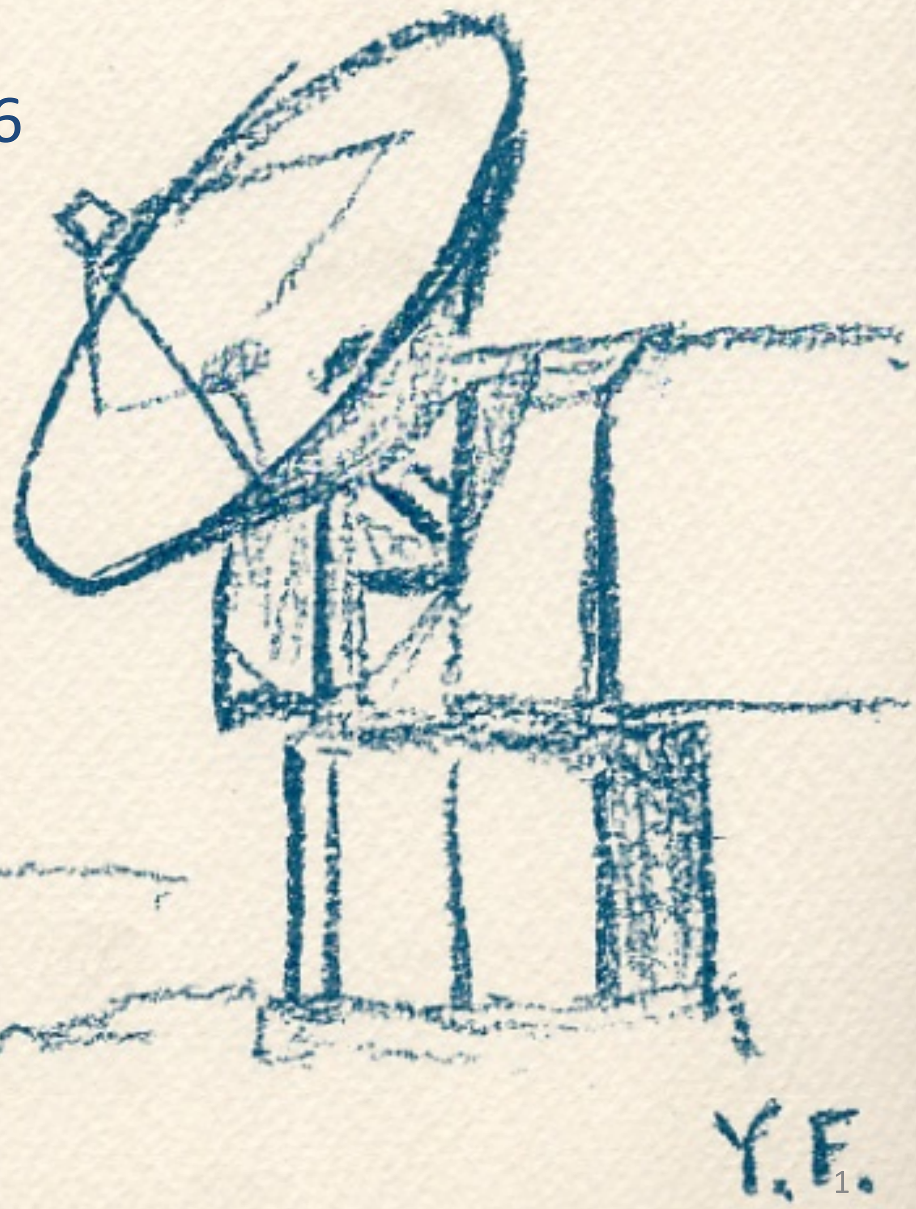


October 13, 2021

# The origin of the Galactic cosmic rays

1912 Discovery of the cosmic rays by V. Hess

Cosmic ray protons are not easily identified
Interaction with low energy protons allows to probe CRs
– p-p collision creates pions, $\pi^0$, $\pi^+$, $\pi^-$
  $\pi^0$ decays into two <u>gamma rays</u>
  $\pi^+$, $\pi^-$ decay and produce <u>neutrinos</u>

Two possible <u>gamma ray origins</u> must be disentangled
– hadronic : p-p collision
  CR protons produce gamma rays via neutral pion
  CRp+p→$\pi^0$→$2\gamma$
– leptonic : inverse Compton scattering
  CR electrons scatter low-energy photons(CMB)→ $\gamma$

Verification of the hadronic gamma rays is the key for the cosmic ray origin and calculated CR proton energy can test CR budget in our Galaxy

The Galactic Plane H.E.S.S. TeV gamma rays (2018)

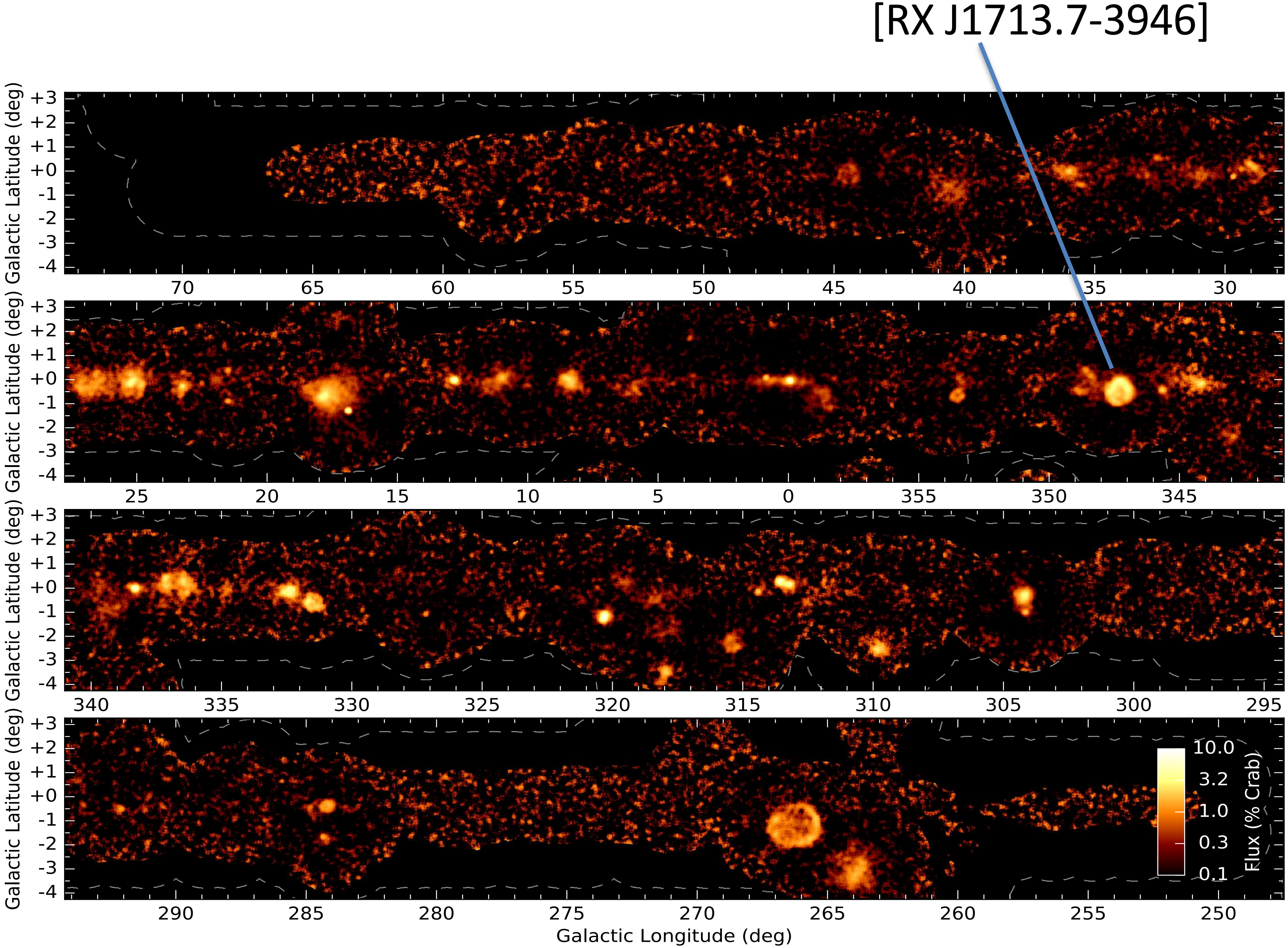

# SNRs emitting gamma-rays

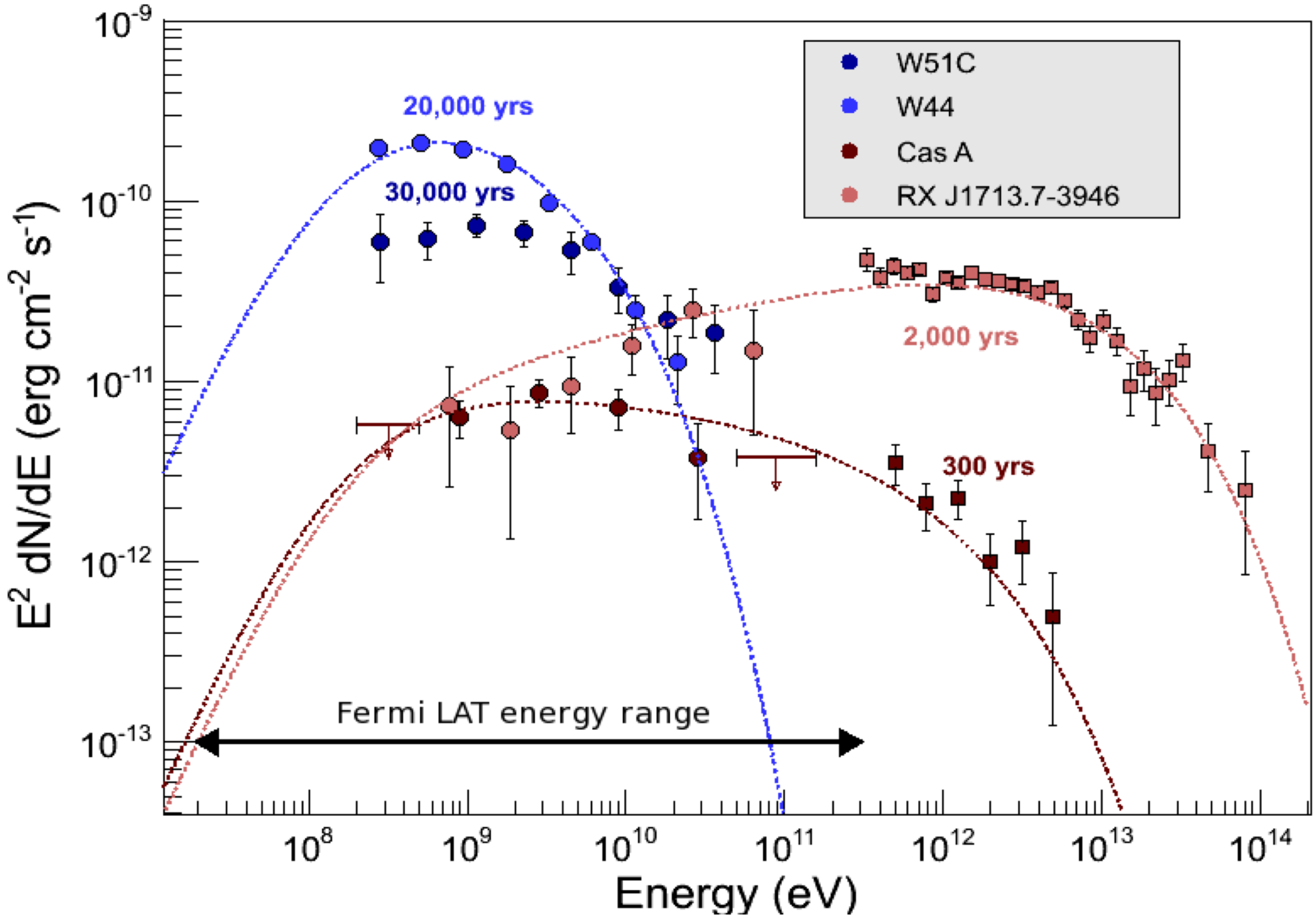


Courtesy H. Tajima

## Key observable quantities of young supernova remnants

SNR as the best candidate where DSA is working to accelerate CRs
RX J1713.7-3946 the brightest gamma ray SNR, most promising object

Gamma rays (Ng in count);
GeV-TeV gamma rays observed with HESS, Veritas, MAGIC, Fermi, AGILE …

X rays (Nx in count);
Non-thermal X rays observed with Suzaku, XMM Newton, Chandra….

Interstellar protons (Np in column density);
NANTEN 4m telescope, Mopra 22 m telescope, ATNF etc.

# NANTEN & NANTEN2

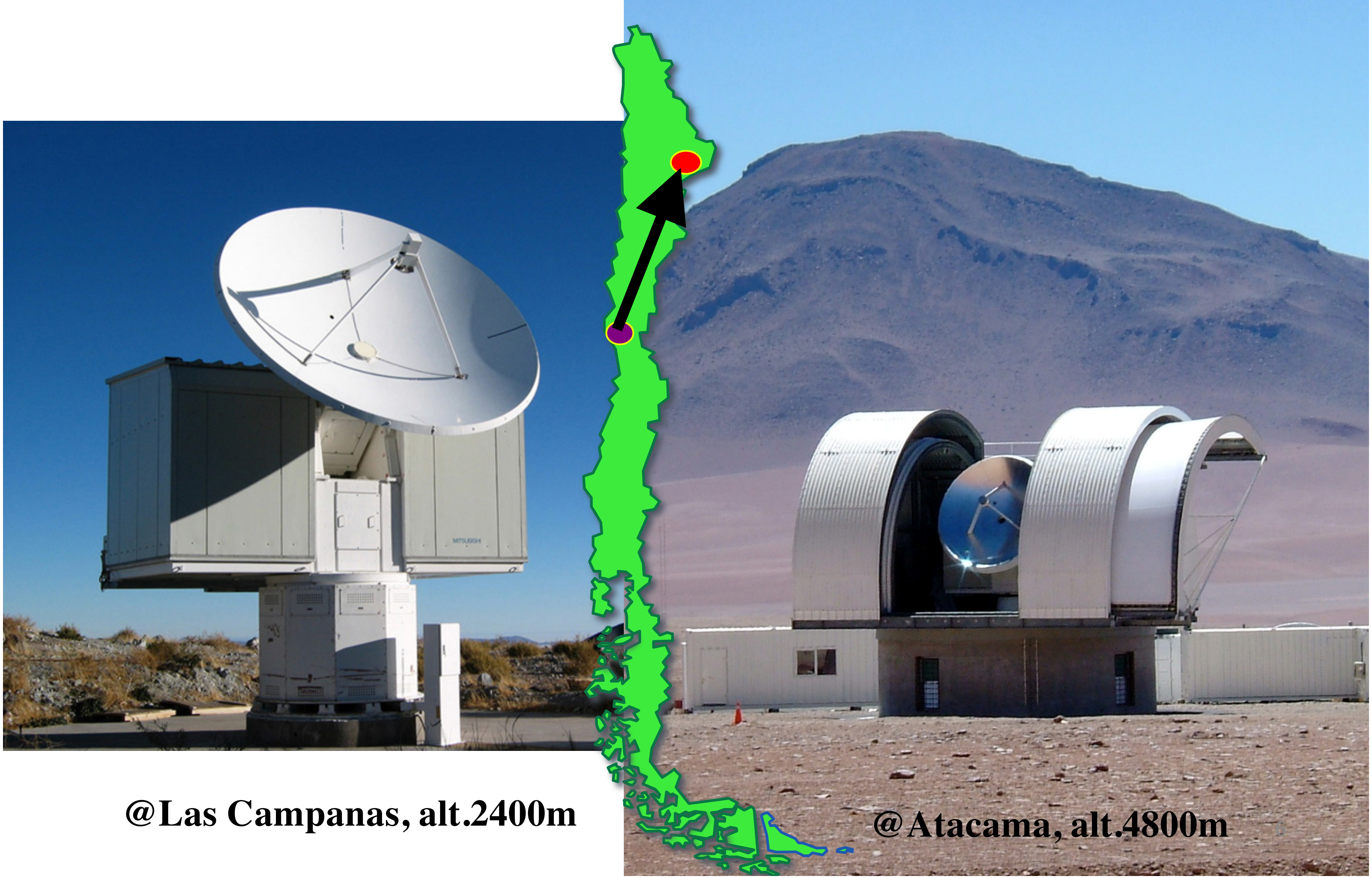

# H.E.S.S. TeV gamma rays vs. CO(J=1-0):

## small CO telescope is powerful for comparison with gamma rays

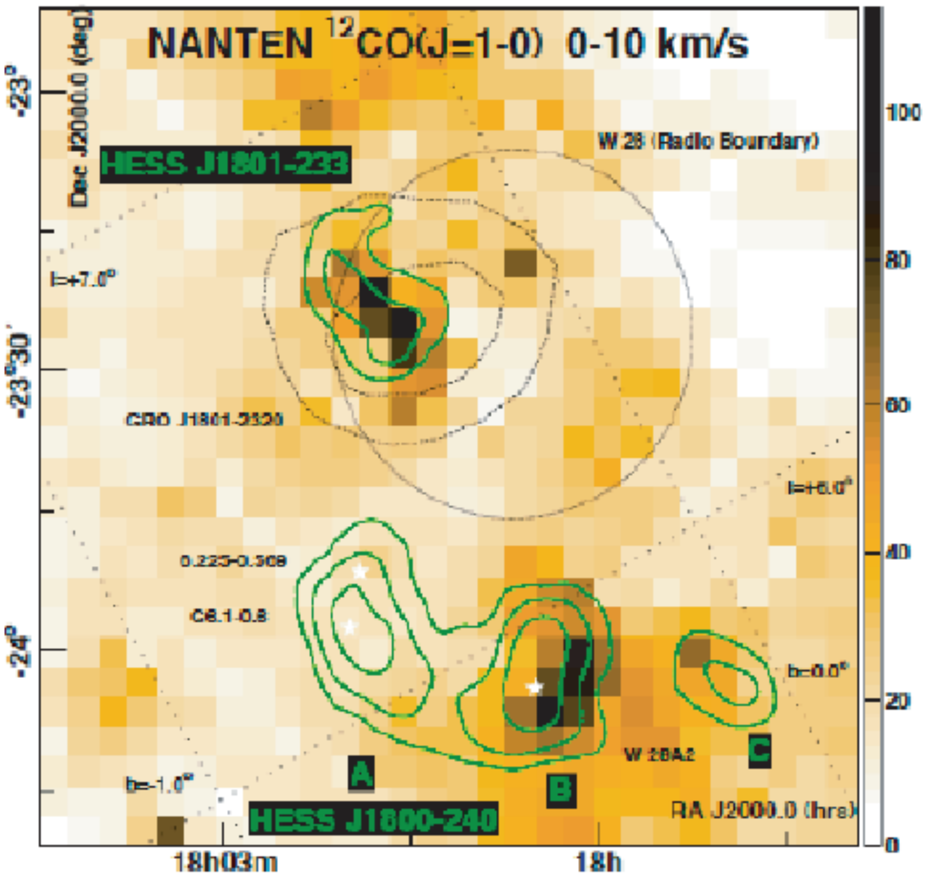


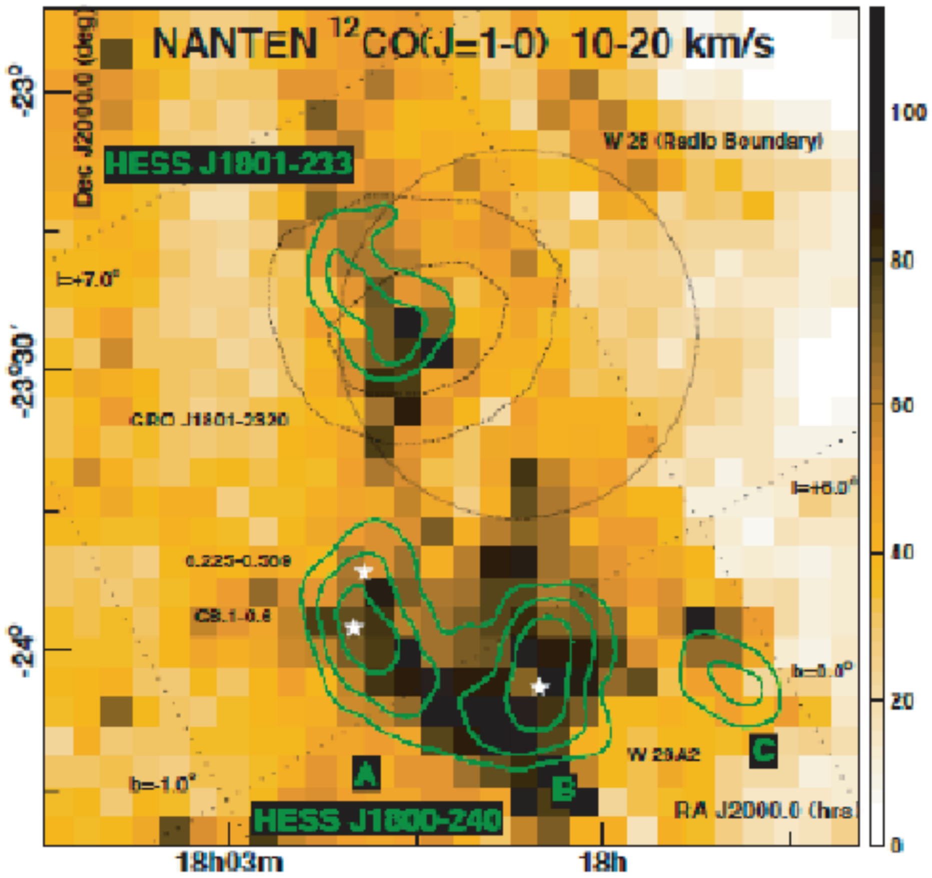


**Left: NANTEN 12CO(1-0) image (beam size : 2.7’) of the W 28 region for VLSR=0 to 10 km/s with H.E.S.S. VHE γ ray significance contours overlaid (green) -levels 4,5,6σ. The radio boundary of W 28, the 68% and 95% location contours of GRO J1801－2320 and the location of the HII region W 28A2 (white stars) are indicated.**
**Right: NANTEN 12CO(1-0) image for VLSR=10 to 20 km/s.**

**(Aharonian, Fukui, Moriguchi et al. 2007)**

# RX J1713.7-3946, non-thermal X rays + gamma rays

## First detection of CO associated

[-11 km/s < $V_{LSR}$ < -3 km/s, distance 1kpc]

magenta NANTEN CO, grey ASCA X rays

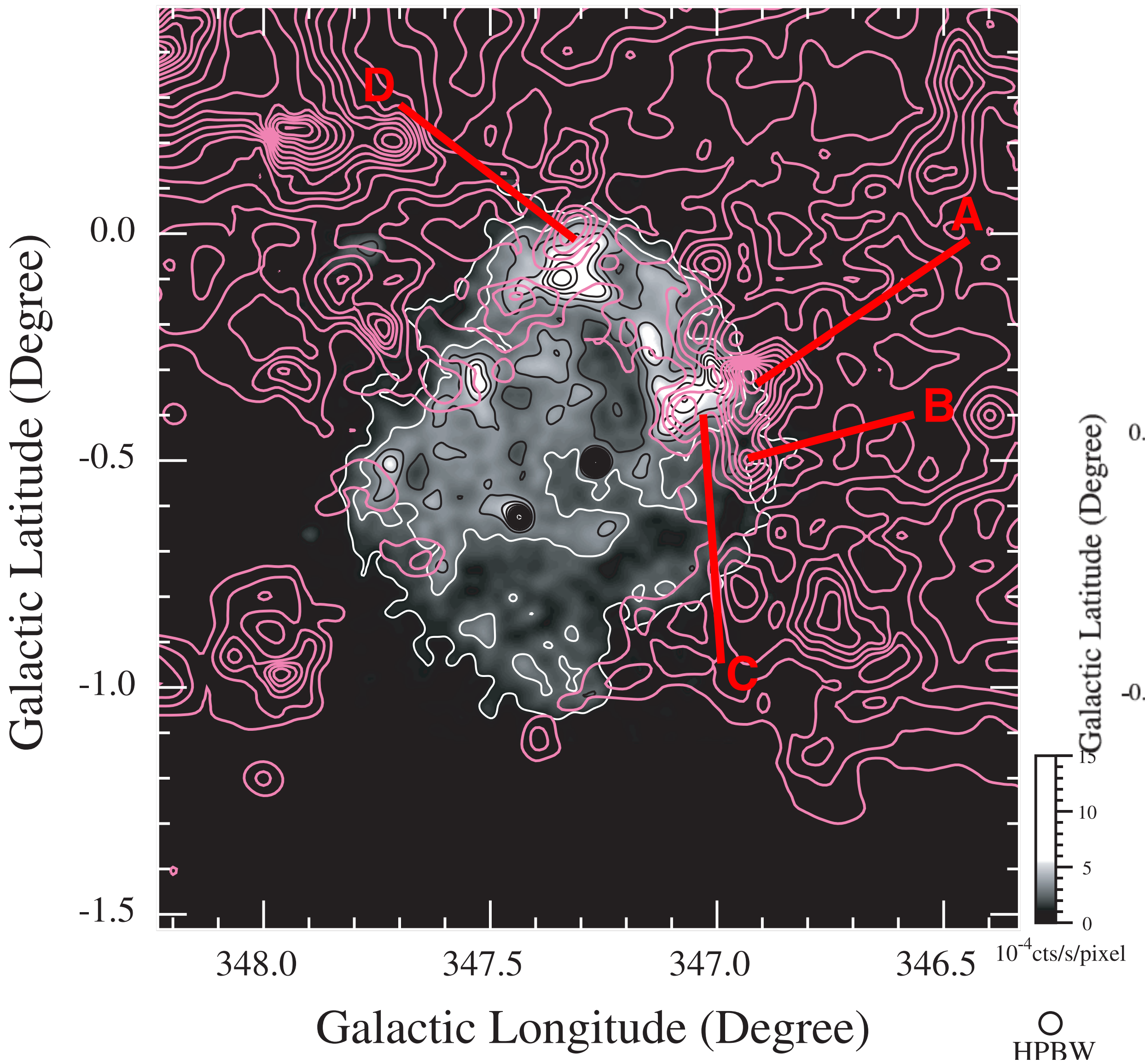


yellow TeV gamma-rays
Enomoto+ 2002

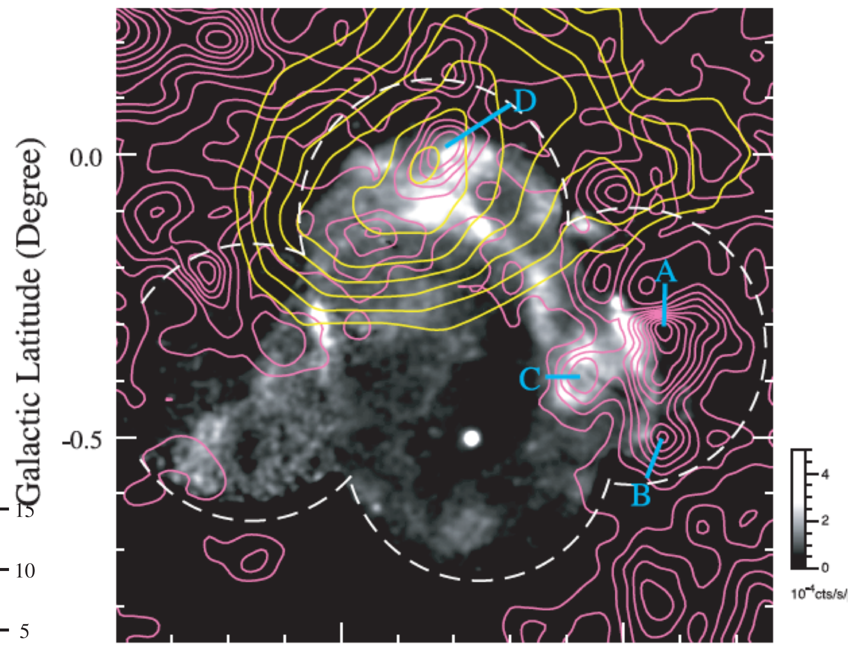


Fukui et al. 2003

# RX J1713 distance 1 kpc

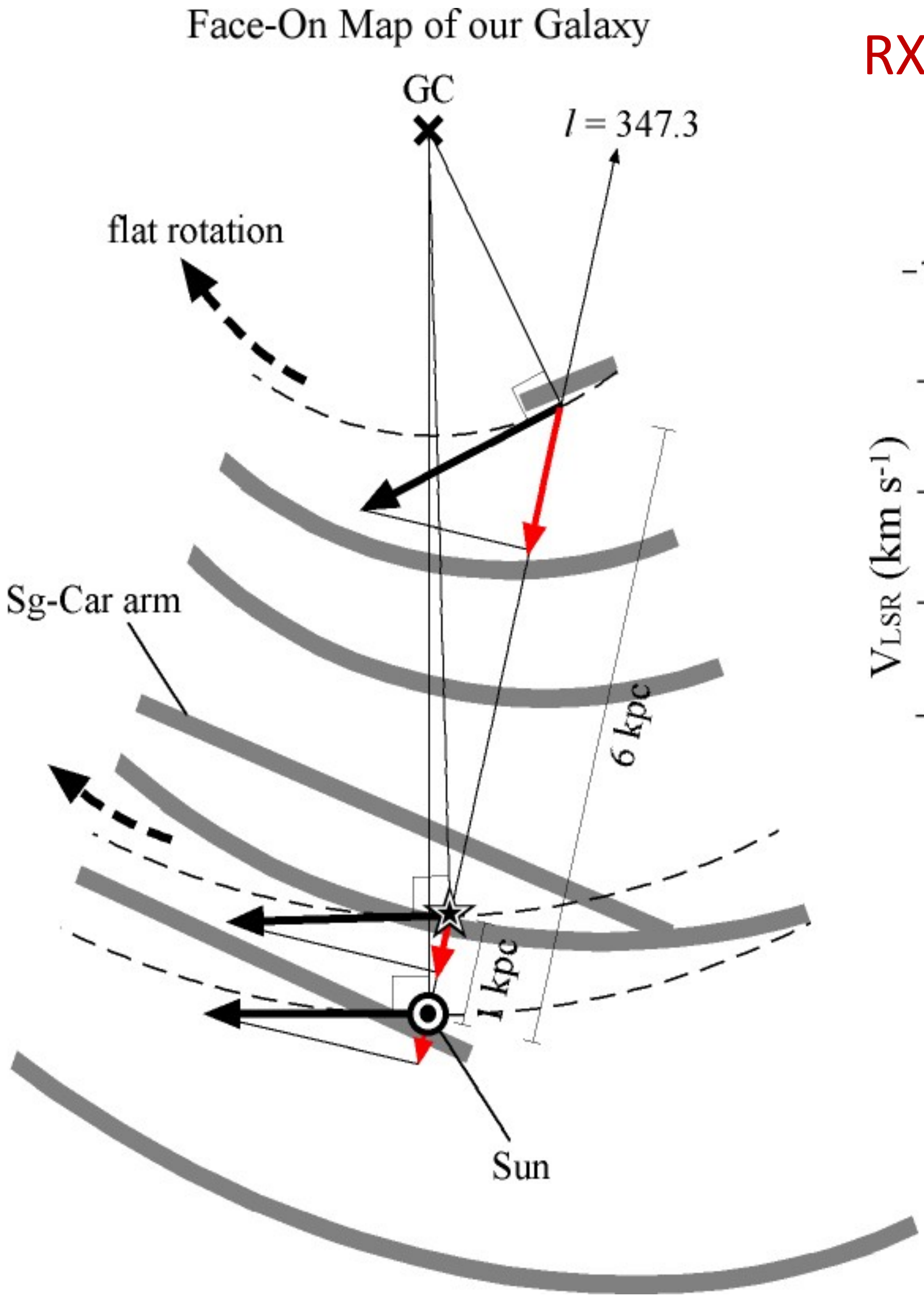


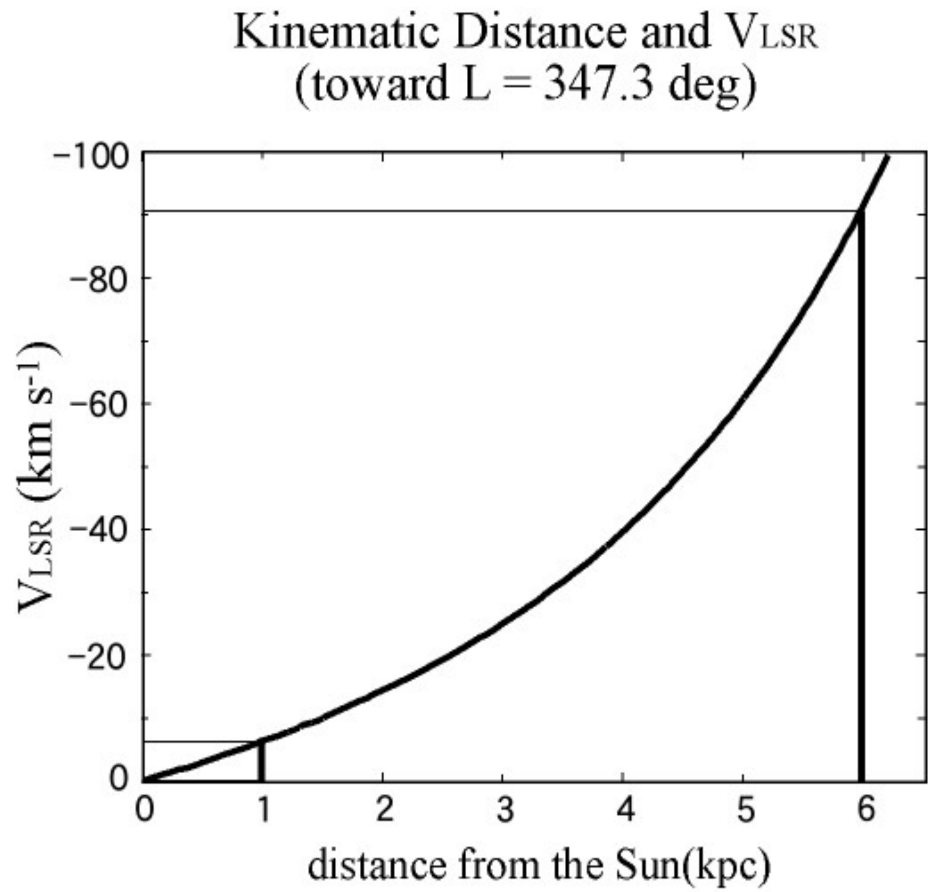


Fukui et al. 2003

# RXJ1713 gamma-ray shell by H.E.S.S.

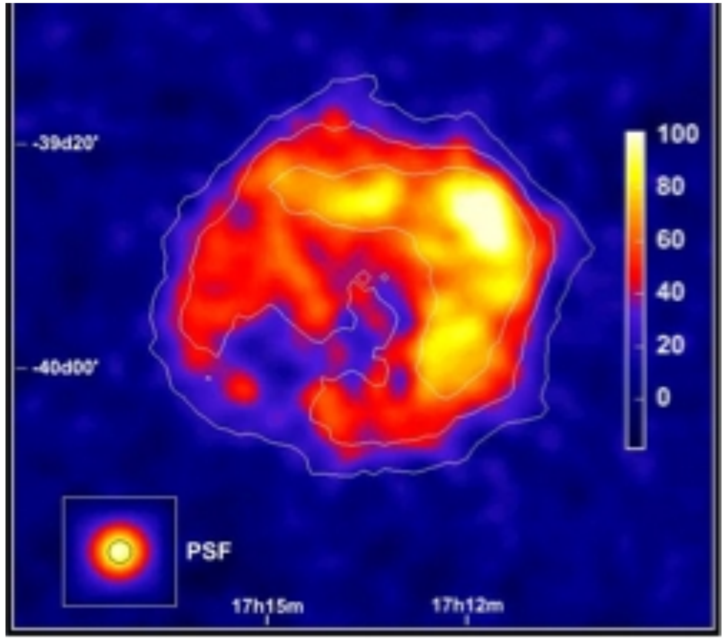


- TeV gamma ray shell-like structure: similar to X-rays
- No significant variation of spectrum index across the regions
- spatial correlation with surrounding molecular gas
- the correlation seems not complete

Aharonian+ 2006

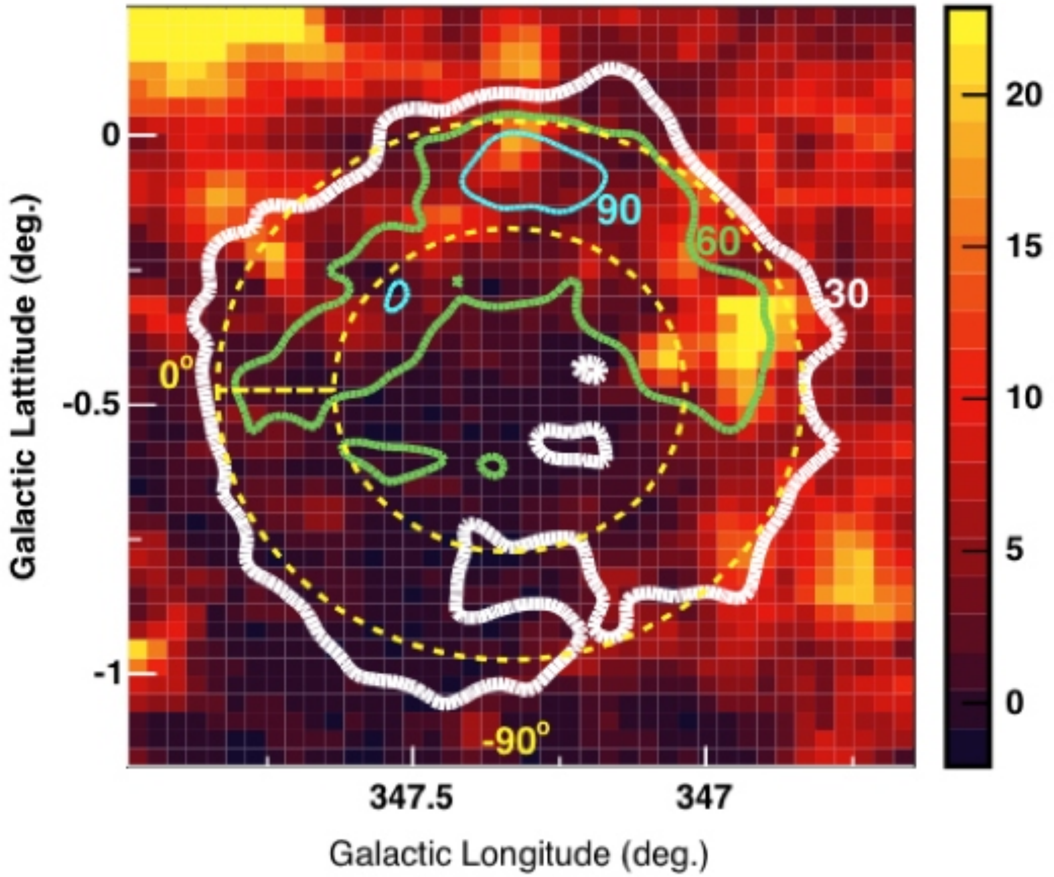


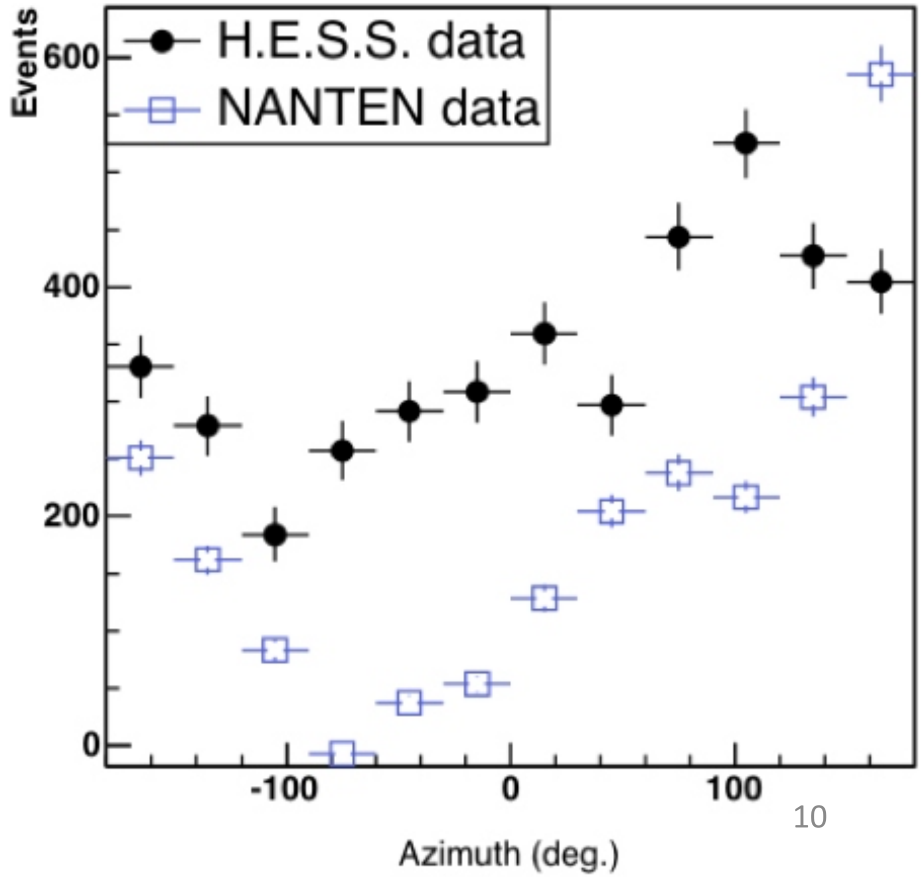

# RX J1713.7-3946

"True interstellar proton is not given by CO alone.
HI can be as dense as 100 $cm^{-3}$."

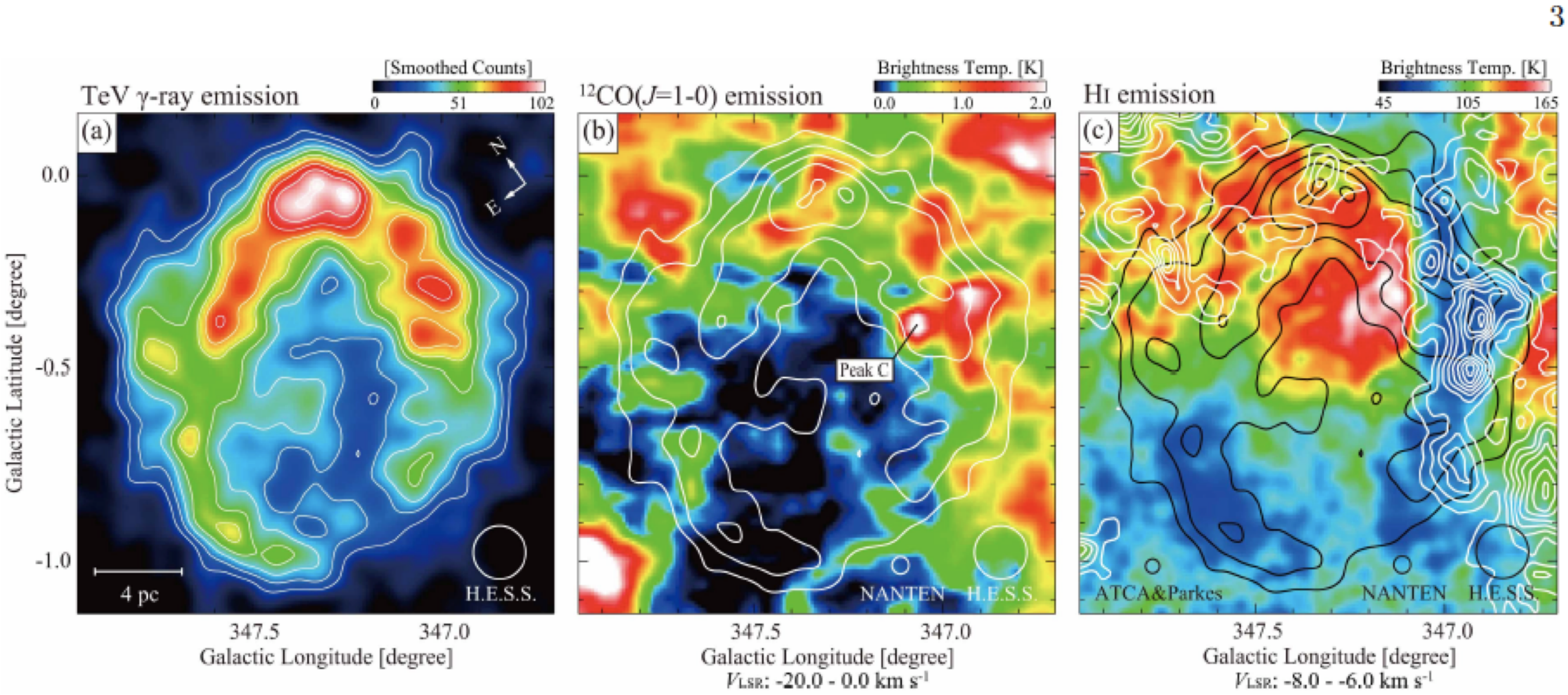


H.E.S.S. TeV gamma rays NANTEN CO ATNF HI

Fukui et al. 2012, ApJ, 746, 82

# Interstellar protons HI+$H_2$ in RX J1713.7-3946 very similar to TeV gamma rays support hadronic scenario ?

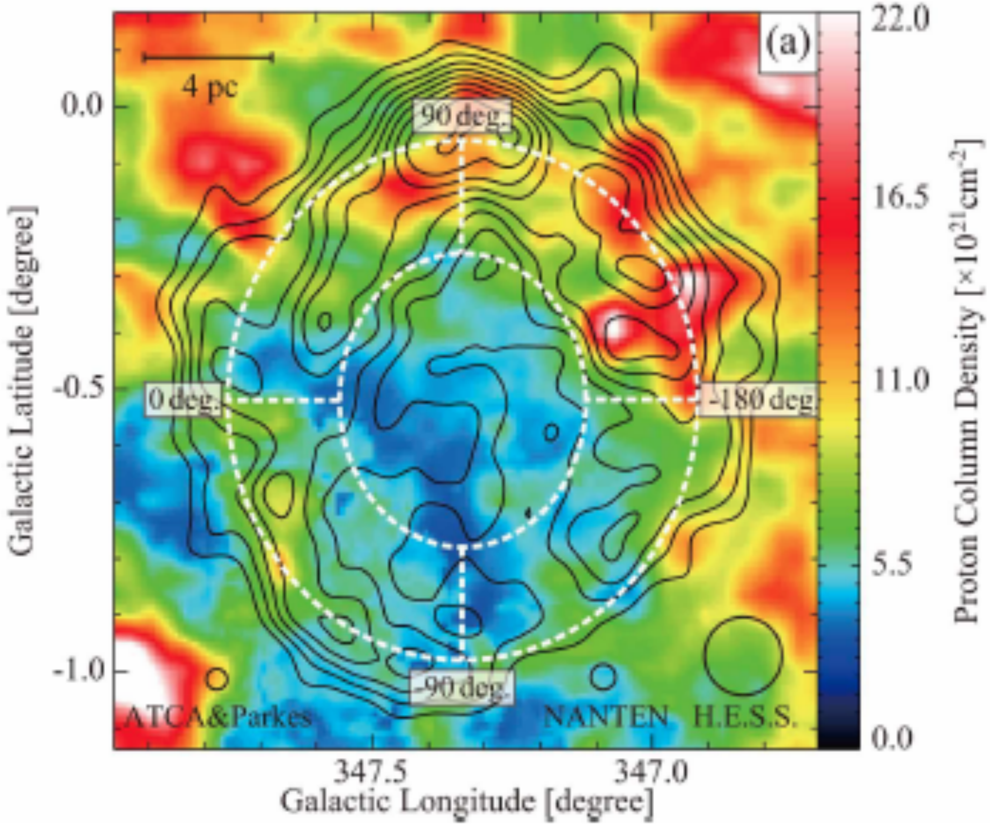


HI + $2H_2$

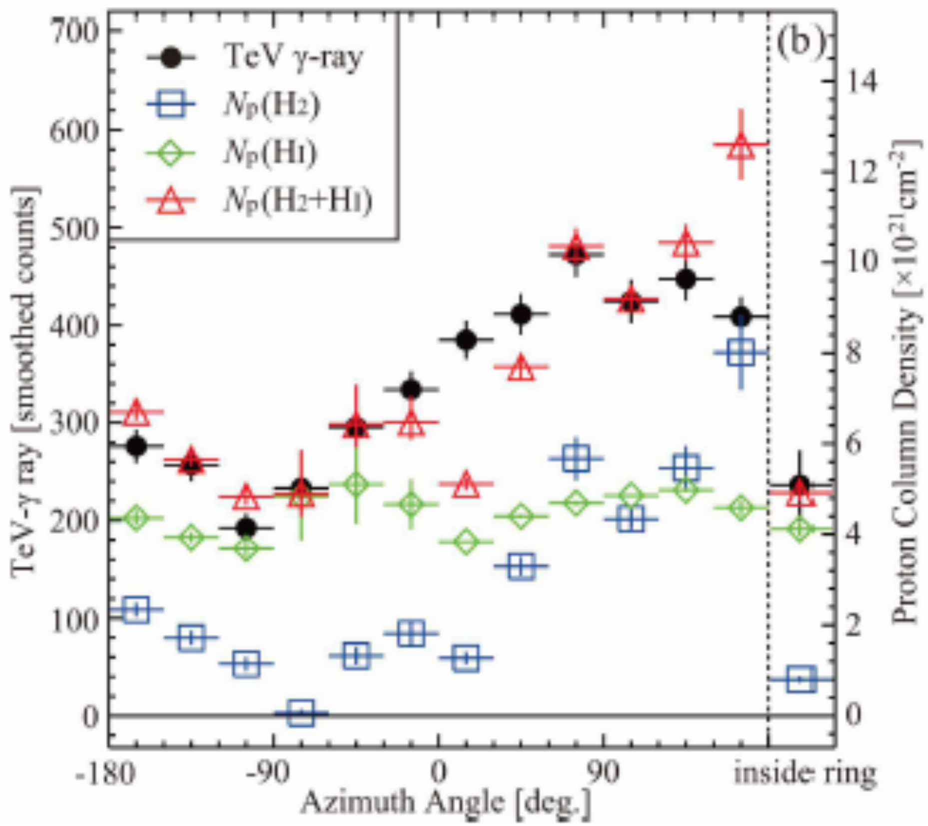


Fukui et al. 2012

# Leptonic dominant broad band spectrum

## Zirakashvili & Aharonian 2010 ApJ 708, 965Z

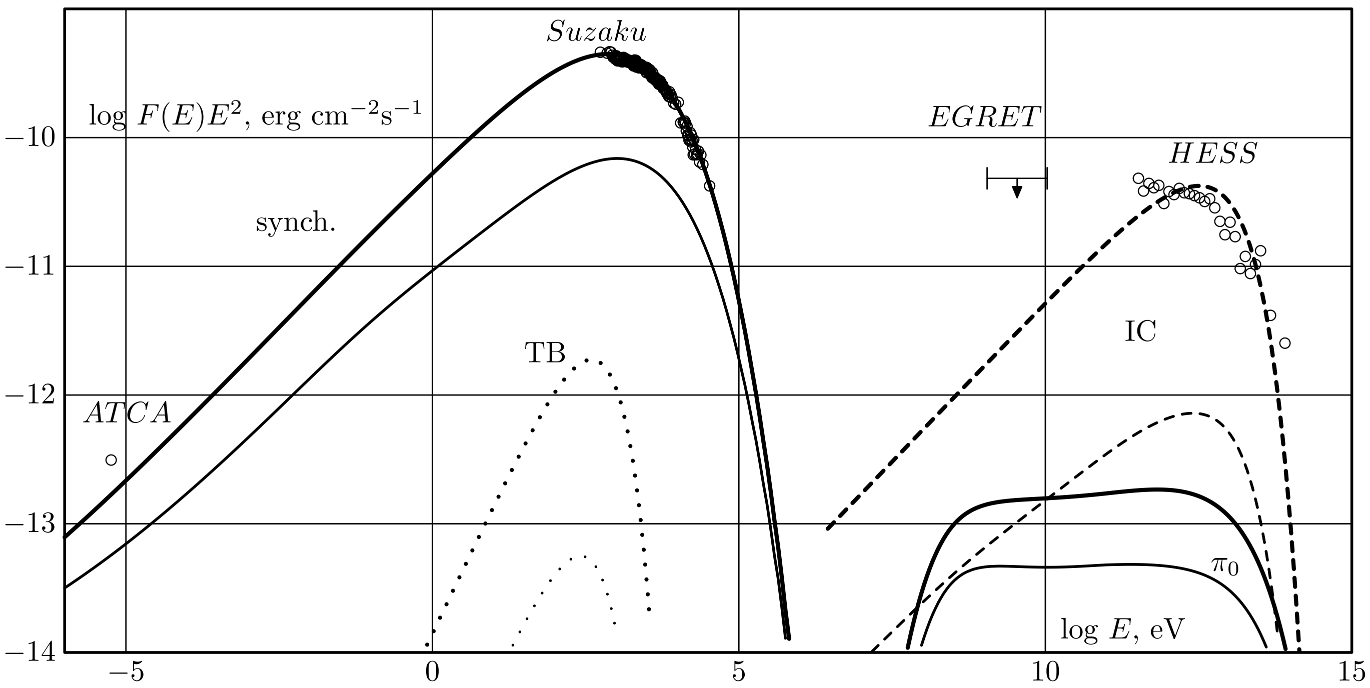


Fig. 8.— Broad-band emission of RX J1713.7-3946 for the leptonic scenario of gamma-rays with a non-modified forward shock. The principal model parameters are: $t = 1620$ yr, $D = 1.5$ kpc, $n_H$ =0.02 cm$^{-3}$, $E_{SN} = 1.2 \cdot 10^{51}$ erg, $M_{ej} = 0.74 M_{\odot}$, $M_A^f = 69$, $M_A^b = 10$, $\xi_0 = 0.1$, $K_{ep}^f = 2.3 \cdot 10^{-2}$, $K_{ep}^b = 9 \cdot 10^{-4}$. The calculations lead to the following values of the magnetic fields and the shock speeds at the present epoch: the magnetic field downstream of the forward and reverse shocks $B_f = 17$ $\mu$G and $B_b = 31$ $\mu$G, respectively, the speed of the forward shock $V_f = 3830$ km s$^{-1}$, the speed of the reverse shock $V_b = -1220$ km s$^{-1}$. The following radiation processes are taken into account: synchrotron radiation of accelerated electrons (solid curve on the left), IC emission (dashed line), gamma-ray emission from pion decay (solid line on the right), thermal bremsstrahlung (dotted line). The input of the reverse shock is shown by the corresponding thin lines.

# Key issues to be solved

- Gamma rays are hadronic or leptonic? Interstellar protons show similar distribution to gamma rays, but the non-thermal X rays, too.

- Leptonic gamma rays can be excluded?
  Magnetic field is strong enough to cause significant loss of CR electrons?
  Probably no. See Inoue+ 2012, low B field, less than 100$\mu$G, dominates.

- Cosmic ray protons are excluded from high density cores?
  cf., Penetration depth effect (Gabici+ 2007; Inoue+ 2012; Inoue 2019)

- What can neutrinos tell on the cosmic ray origins?

- We need a new approach to solve these issues;
  Disentangling the two gamma ray origins is required, but has never been done.

# Fukui+ 2012, strength and weakness

- Fukui+ 2012 showed that the interstellar proton distribution is similar to TeV gamma rays. [HI + H2] is essential as target protons.
- Cosmic ray energy, estimated to be ~$10^{48}$ erg, can supply the Galactic cosmic rays, if CR escape and volume filling factor of interstellar protons are taken into account.
- The hadronic gamma ray is consistent with the SNR origin of CRs, but is not conclusive.
- Resolution is low, ~4 pc. Number of pixels is 10-20 (best data in 2008).
- Significant contribution of the leptonic origin is not excluded.

# Fukui+ 2021, the present work

TeV gamma rays (HESS Collaboration 2018) resolution 4pc→1.4pc

Assumption: gamma rays **Ng** are combination of hadronic and leptonic components in each pixel;

Hadronic Ng is proportional to target protons **Np**

Leptonic Ng is proportional to non-thermal X ray count **Nx**

**Ng** (count) = a **Np** ($cm^{-2}$) + b **Nx** (count) : [hadronic]＋[leptonic]

- a: cross section of pp reaction, cosmic ray proton density
- b: inverse Compton scattering, depends on $B^{-2}$

## Expressions of a and b ( courtesy Ryo Yamazaki, Aoyama Gakuin U.)

- hadronic-γ
  - $\nu\varepsilon_\nu{}^{\mathrm{hadronic}} \sim (n_H \sigma_{\mathrm{pp}} c)\rho_{\mathrm{p}} f$

    CR proton energy
  - $\nu S_\nu{}^{\mathrm{hadronic}} \sim \frac{c\sigma_{\mathrm{pp}}}{4\pi}(n_{\mathrm{H}} l)\rho_{\mathrm{p}} f$

    $= N_{\mathrm{p}}$

    $f = f(P.E_{\mathrm{max,p}}) \sim 1$
- leptonic-γ
  - $\frac{(\nu\varepsilon_\nu{}^{\mathrm{IC}})_{\mathrm{peak}}}{(\nu\varepsilon_\nu{}^{\mathrm{syn}})_{\mathrm{peak}}} \sim \left(\frac{B_{\mathrm{CMB}}}{B}\right)^2$
  - $\nu S_\nu{}^{\mathrm{leptonic}} \sim \frac{l}{4\pi}\nu\varepsilon_\nu{}^{\mathrm{syn}} \left(\frac{B_{\mathrm{CMB}}}{B}\right)^2 g$

    $= N_{\mathrm{x}} h\nu_{\mathrm{x}}$

    $g = g(P.E_{\mathrm{max,e}}) \leftarrow \Gamma_{\mathrm{x}}$
- total-γ
  - $\nu S_\nu \sim \frac{c\sigma_{\mathrm{pp}}}{4\pi}\rho_{\mathrm{p}} f N_{\mathrm{p}} + (h\nu_{\mathrm{x}})\left(\frac{B_{\mathrm{CMB}}}{B}\right)^2 g N_{\mathrm{x}}$

    $\sim N_{\mathrm{g}} h\nu_{\mathrm{TeV}}$ $= a$ $= b$

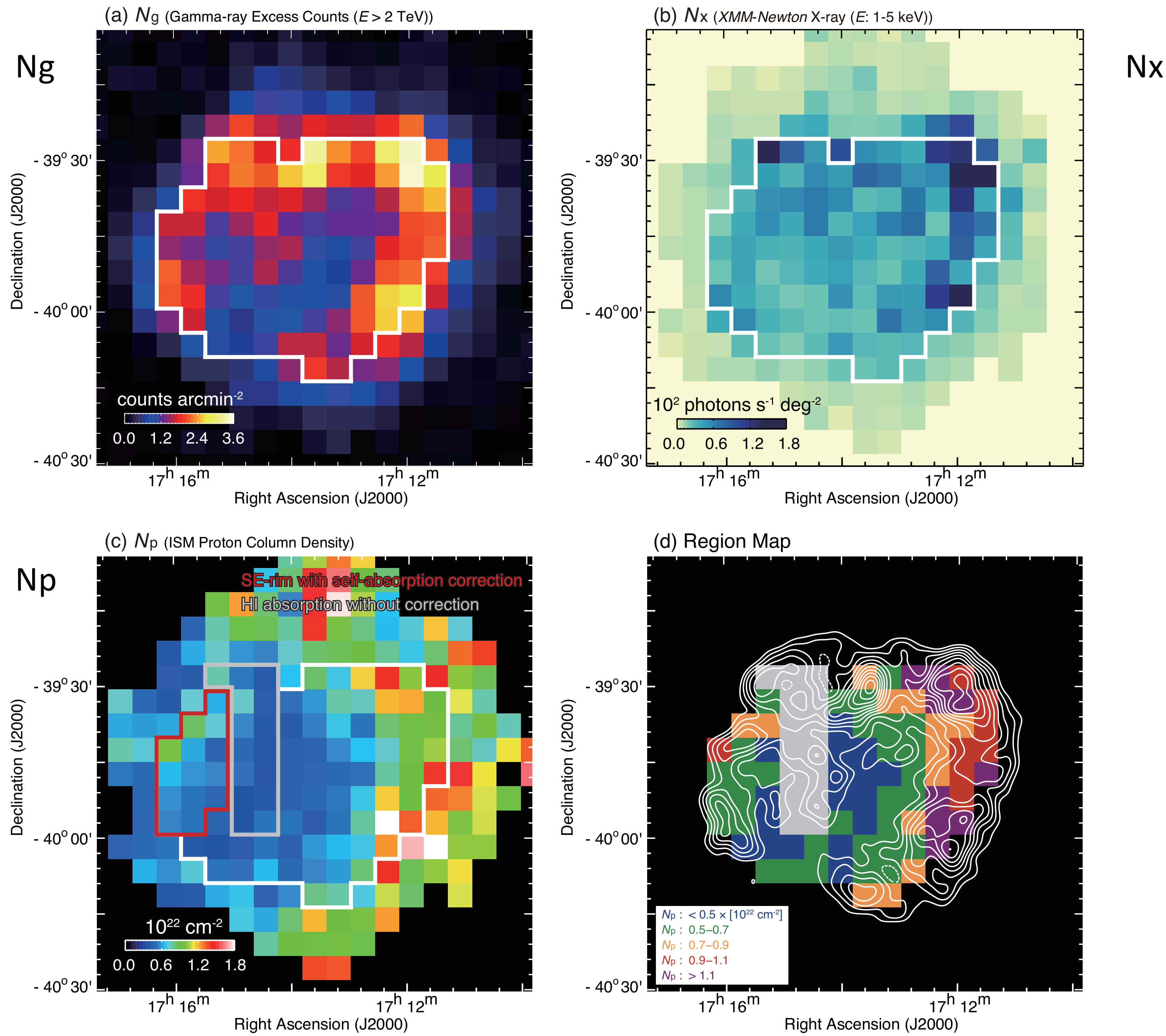

Ng
Nx
Np
(a) Ng (Gamma-ray Excess Counts (E > 2 TeV))
counts arcmin-2
0.0 1.2 2.4 3.6
(b) Nx (XMM-Newton X-ray (E: 1-5 keV))
10² photons s-1 deg-2
0.0 0.6 1.2 1.8
(c) Np (ISM Proton Column Density)
SE-rim with self-absorption correction
HI absorption without correction
10²² cm-2
0.0 0.6 1.2 1.8
(d) Region Map
Np : < 0.5 × [10²² cm-2]
Np : 0.5–0.7
Np : 0.7–0.9
Np : 0.9–1.1
Np : > 1.1
Declination (J2000)
- 39° 30'
- 40° 00'
- 40° 30'
Right Ascension (J2000)
17h 16m
17h 12m

# RX J1713 Np-Nx-Ng correlation

## Np-Ng

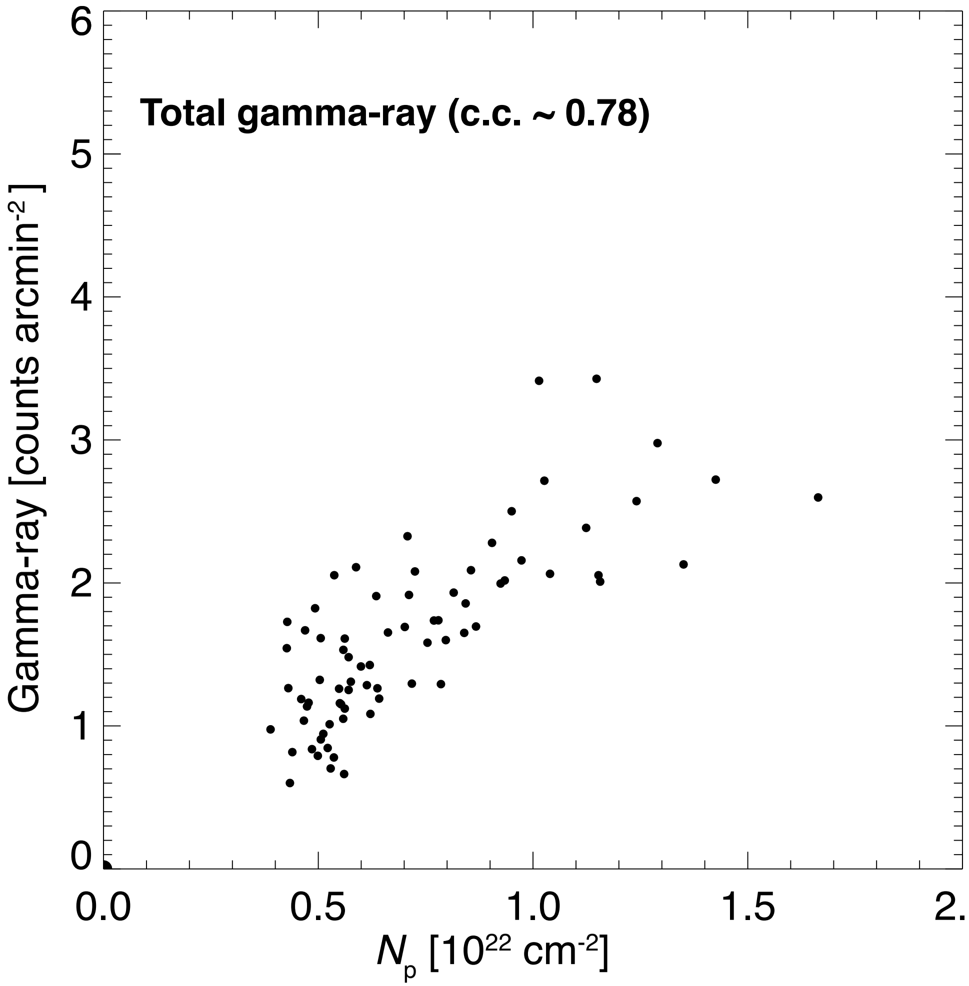


## Nx-Ng

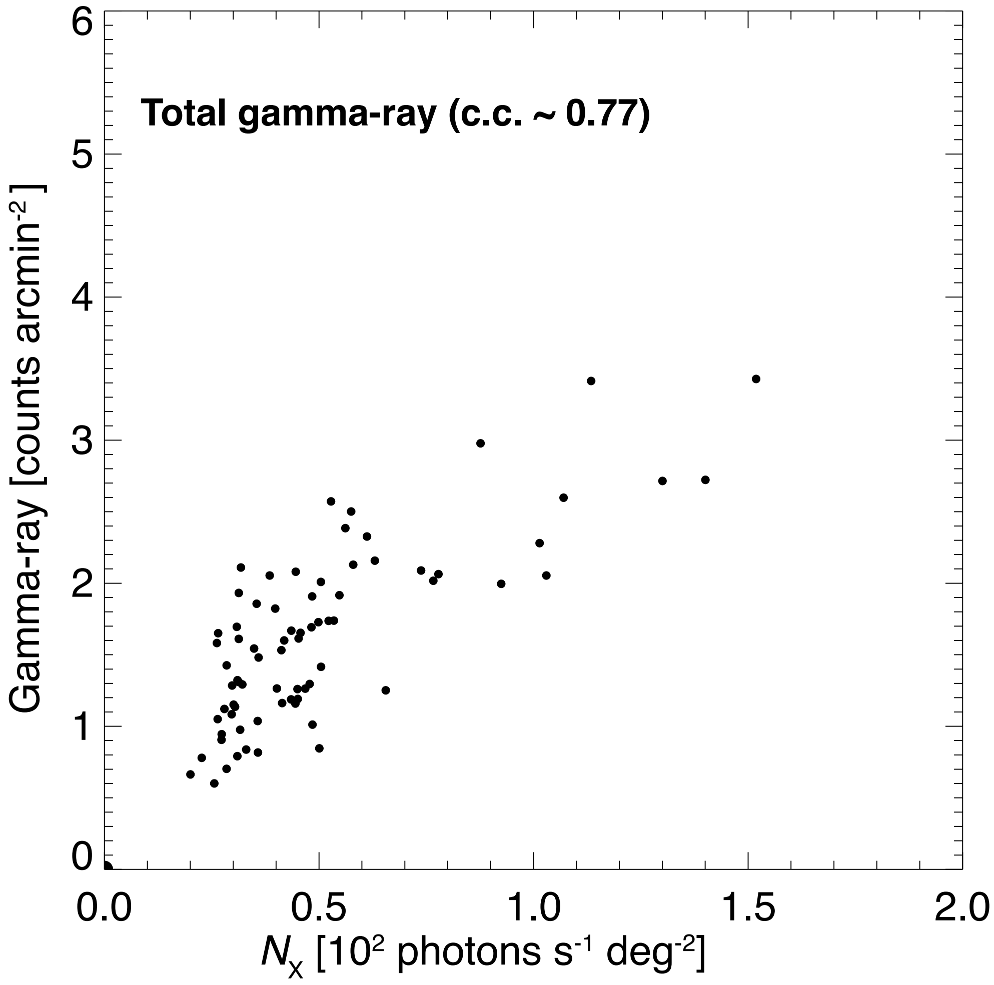

# 3D fit in Np-Nx-Ng space

$$N_g = (1.57 \pm 0.14) \times N_p + (0.91 \pm 0.19) \times N_x$$

Hadronic : Leptonic = 67% : 33%

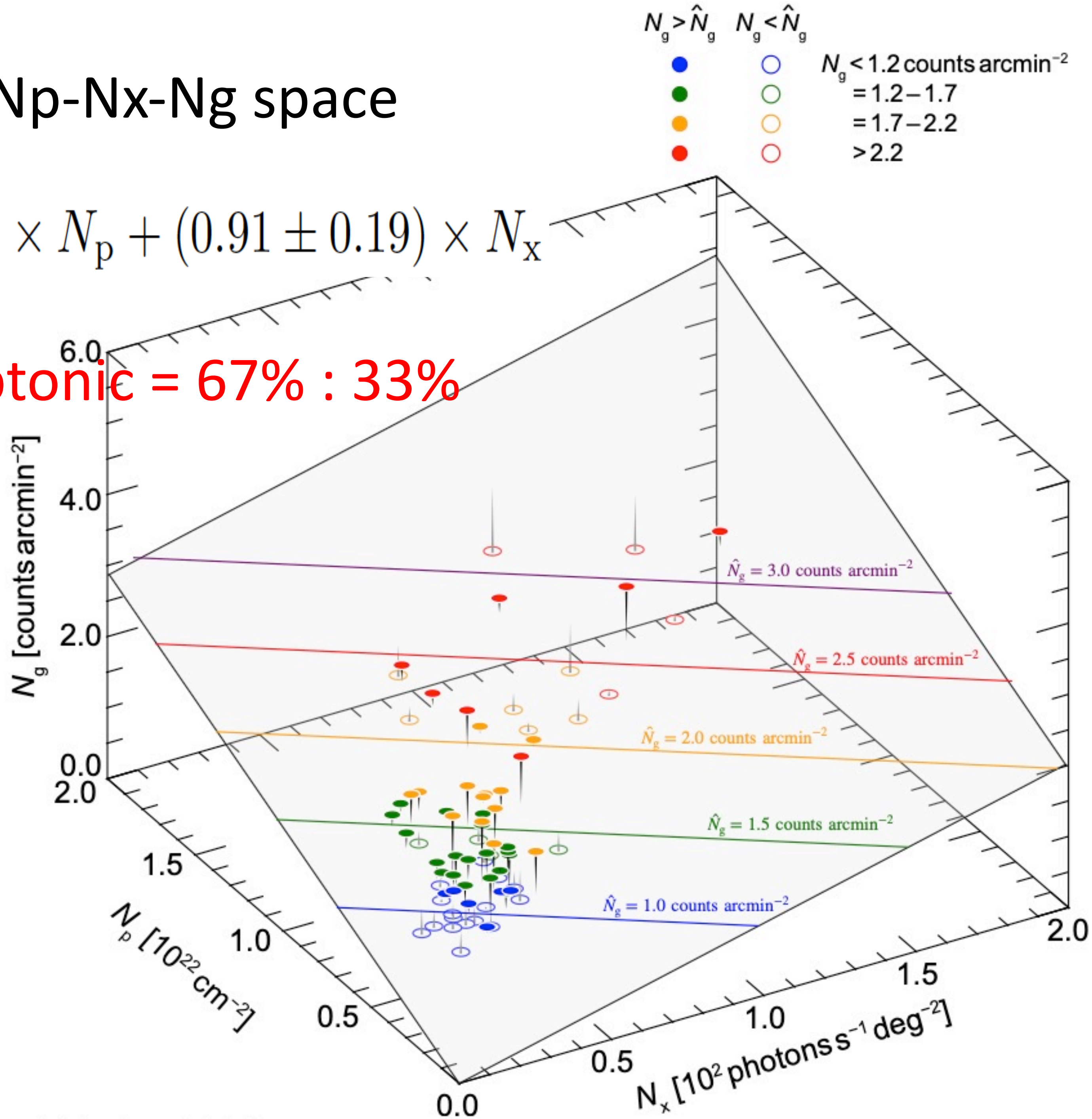


Fukui + 2021

# 3D fit in Np-Nx-Ng space

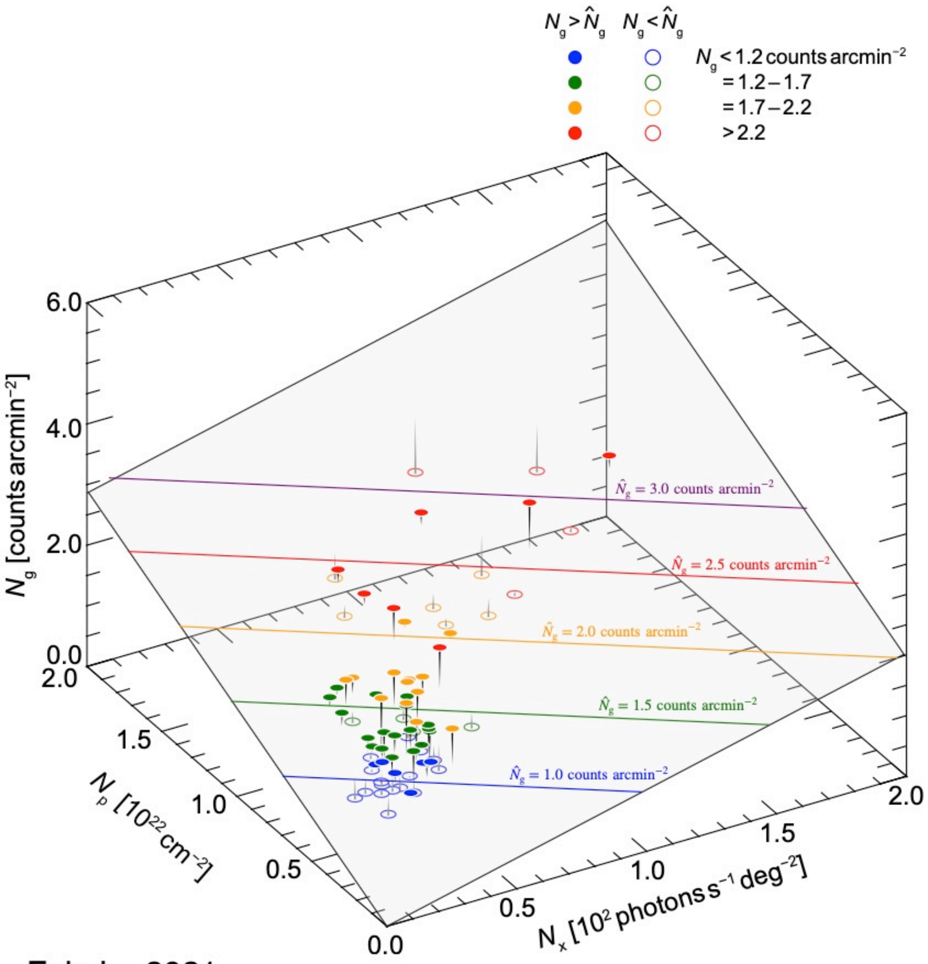


Fukui + 2021

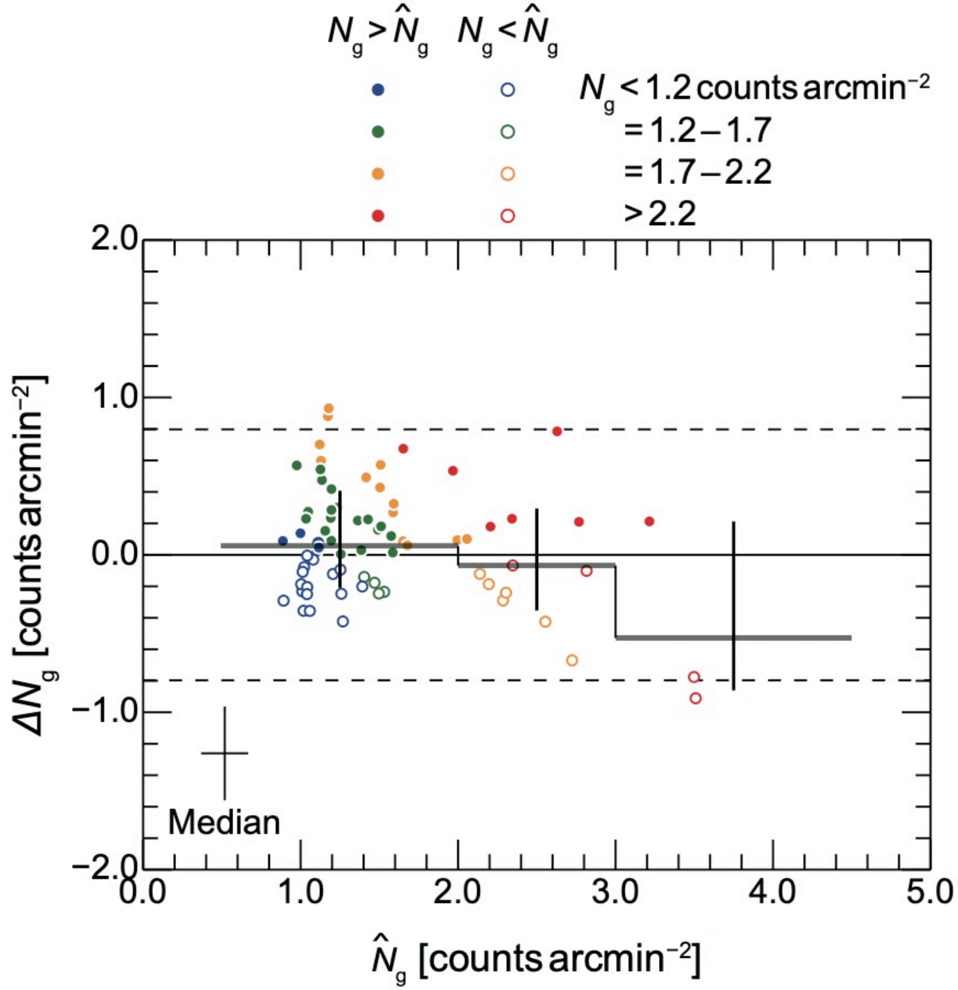

# Hadronic gamma ray count fraction

Contours X rays

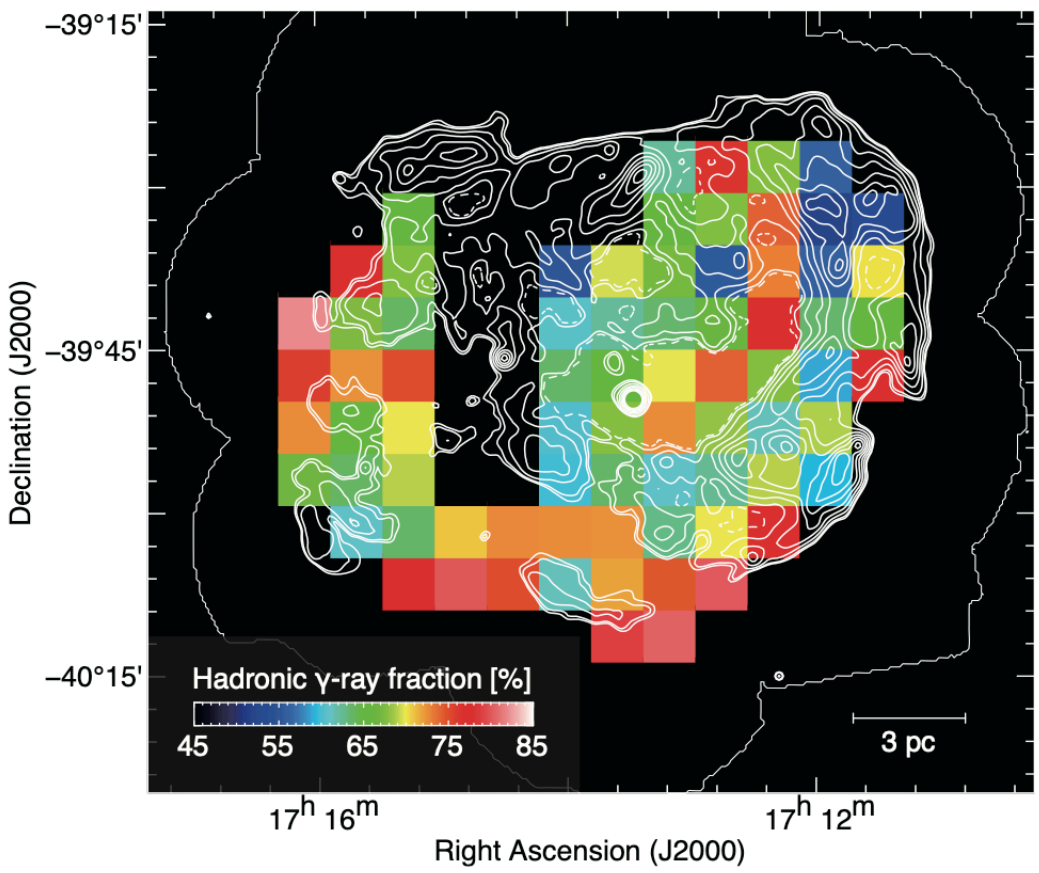


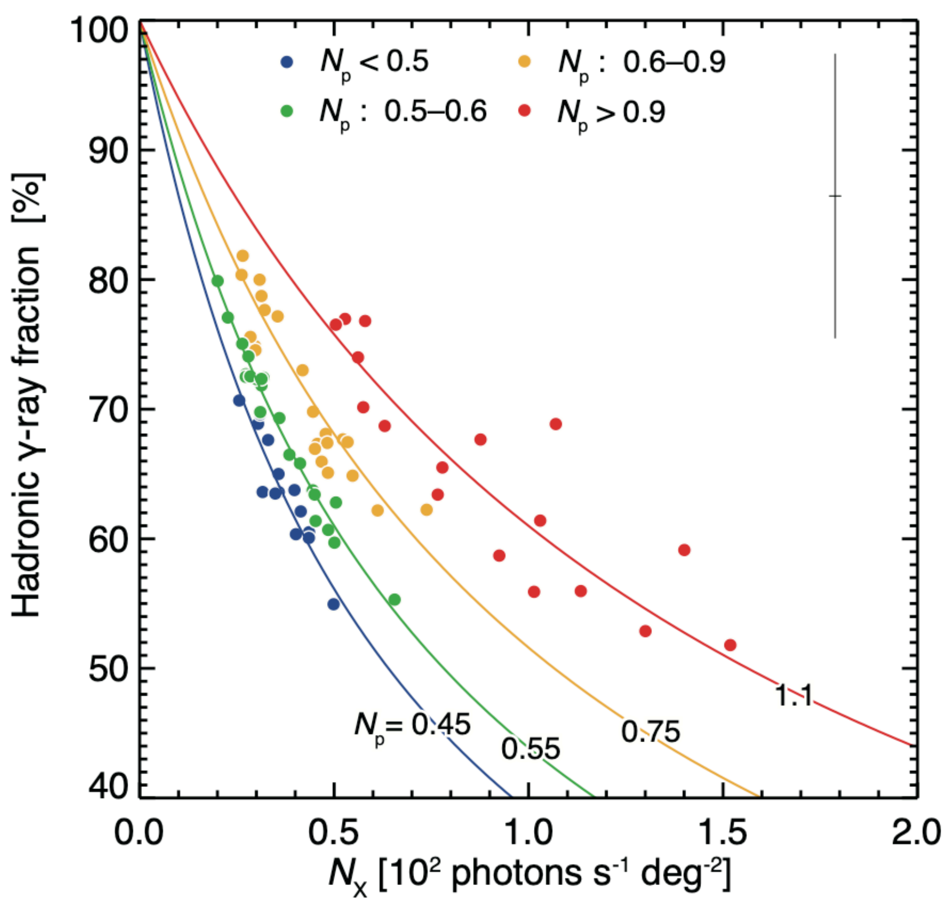

# Different resolutions

**Table 3.** Estimate of the hadronic- and leptonic-origin gamma-rays

| Dataset | | | | Hadronic component | | | Leptonic component | |
|---|---|---|---|---|---|---|---|---|
| Energy band | Pixel size | $\langle \hat{N}_{\rm g} \rangle$ | $\langle N_{\rm p} \rangle$ | $\hat{N}_{\rm g}^{\rm hadronic}$ | $\hat{N}_{\rm g}^{\rm hadronic}/\langle \hat{N}_{\rm g} \rangle$ | $\langle N_{\rm x} \rangle$ | $\hat{N}_{\rm g}^{\rm leptonic}$ | $\hat{N}_{\rm g}^{\rm leptonic}/\langle \hat{N}_{\rm g} \rangle$ |
| (1) | (2) | (3) | (4) | (5) | (6) | (7) | (8) | (9) |
| H.E.S.S.18 | | | | | | | | |
| $E > 2$ TeV | $4'.8$ | $1.56 \pm 0.02$ | 0.72 | $1.04 \pm 0.12$ | $(67 \pm 8)\%$ | 0.50 | $0.51 \pm 0.12$ | $(33 \pm 8)\%$ |
| | $6'.6$ | $1.57 \pm 0.04$ | 0.73 | $1.01 \pm 0.17$ | $(65 \pm 11)\%$ | 0.50 | $0.55 \pm 0.17$ | $(35 \pm 11)\%$ |
| | $8'.4$ | $1.54 \pm 0.07$ | 0.74 | $1.01 \pm 0.21$ | $(66 \pm 14)\%$ | 0.50 | $0.53 \pm 0.20$ | $(34 \pm 13)\%$ |
| $E > 250$ GeV | $6'.6$ | $11.7 \pm 0.3$ | 0.73 | $7.7 \pm 1.2$ | $(66 \pm 11)\%$ | 0.50 | $4.0 \pm 1.2$ | $(34 \pm 10)\%$ |
| | $8'.4$ | $11.7 \pm 0.4$ | 0.74 | $7.6 \pm 1.3$ | $(65 \pm 11)\%$ | 0.50 | $4.0 \pm 1.3$ | $(35 \pm 11)\%$ |
| H.E.S.S.07 | | | | | | | | |
| $E \gtrsim 300$ GeV | $8'.4$ | $1.92 \pm 0.06$ | 0.74 | $1.38 \pm 0.20$ | $(72 \pm 11)\%$ | 0.50 | $0.54 \pm 0.20$ | $(28 \pm 10)\%$ |

NOTE— Columns (1) and (2): energy band and pixel size of the dataset, (3), (4) and (7): spatial averages of observed $N_{\rm g}$ (counts arcmin$^{-2}$), $N_{\rm p}$ ($10^{22}$ cm$^{-2}$) and $N_{\rm x}$ (photons s$^{-1}$ degree$^{-2}$), (5) and (8): predicted values of hadronic- and leptonic-origin gamma-rays (counts arcmin$^{-2}$), (6) and (9): fraction of the hadronic and leptonic components.

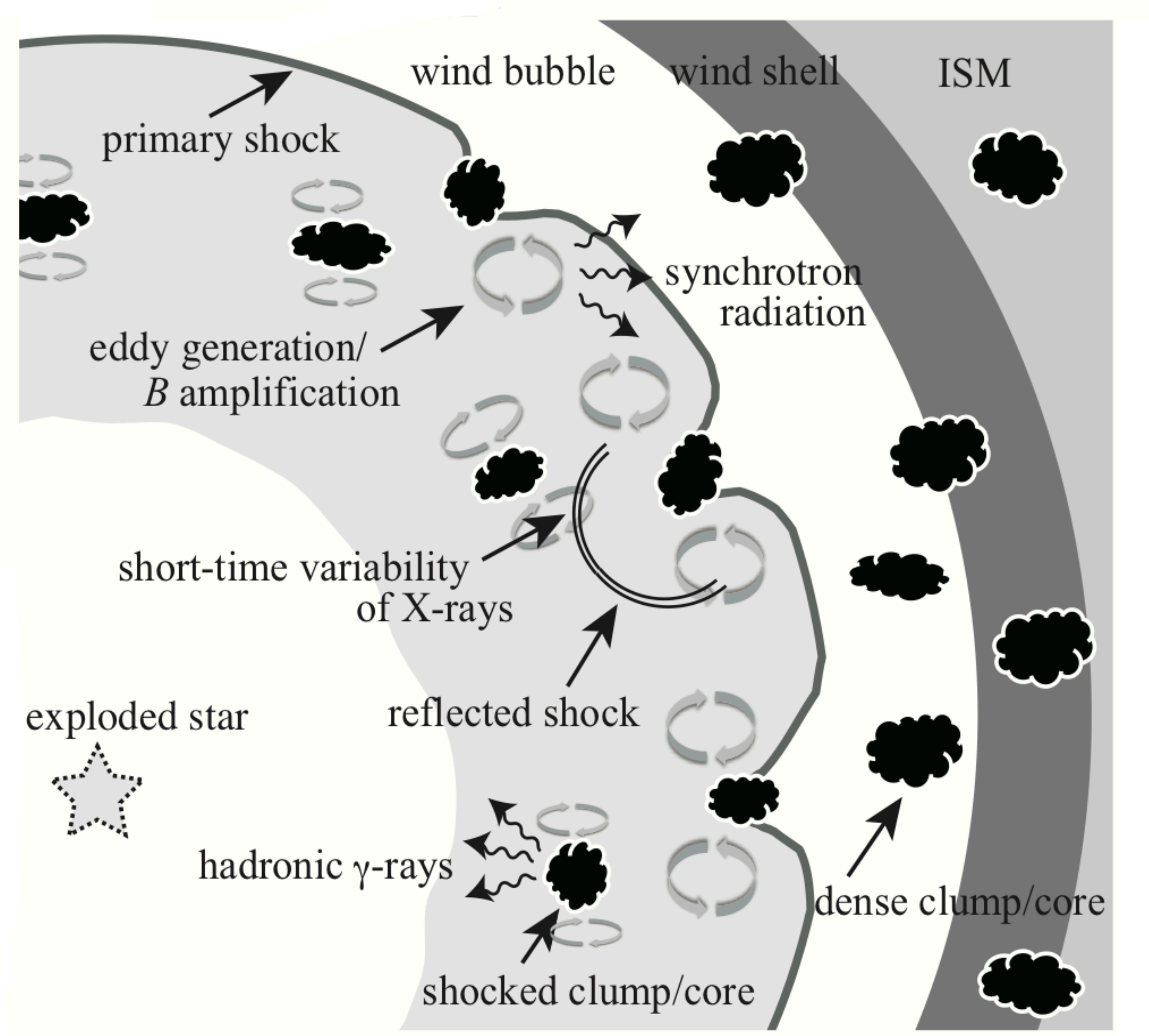
wind bubble
wind shell
ISM
primary shock
synchrotron
radiation
eddy generation/
*B* amplification
short-time variability
of X-rays
reflected shock
exploded star
hadronic γ-rays
dense clump/core
shocked clump/core

Inoue+ 2012

# Penetration depth of CR protons

CR protons cannot penetrate into dense cloud cores (e.g., Maxted+ 2013)
The densest core C may show gamma ray decrease (Inoue+ 2012, see also Gabici+ 2007)

$$l_{\rm pd}\ ({\rm pc}) = 0.1\ \eta^{1/2} \left(\frac{E}{10\ {\rm TeV}}\right)^{1/2} \left(\frac{B}{100\ \mu G}\right)^{-1/2} \left(\frac{t_{\rm age}}{10^3\ {\rm yr}}\right),$$

13

(b) Gamma-ray ($E > 250$ GeV)

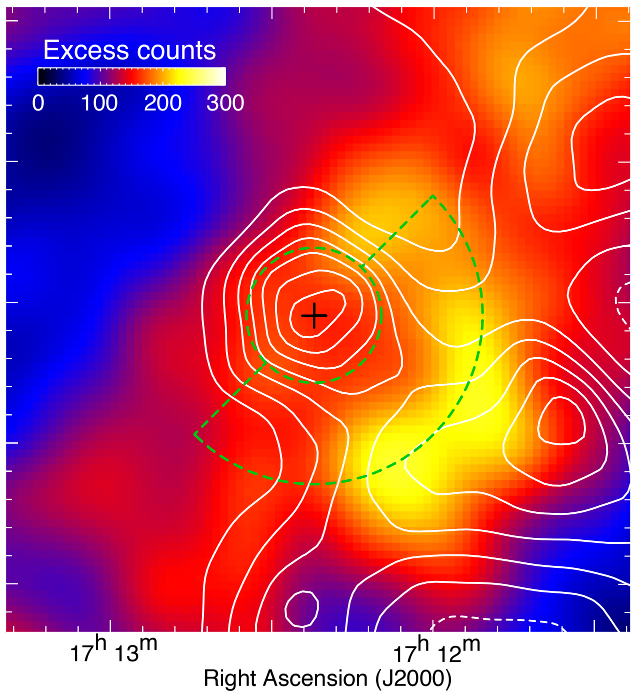


(c) Radial profiles

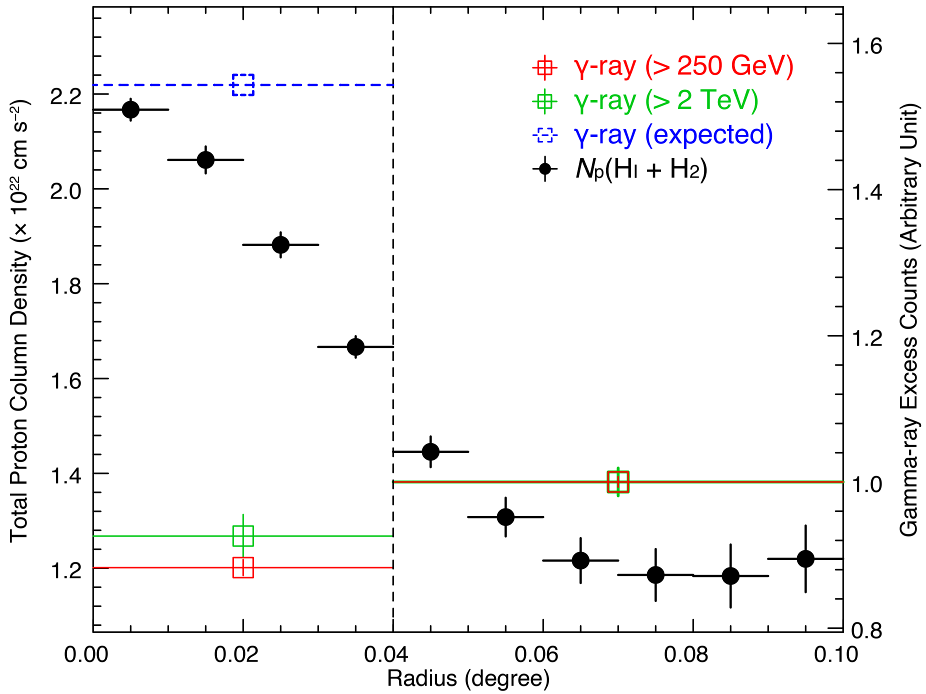

# Shock cloud interaction
# X rays are enhanced around dense cores
# Sano+ 2013

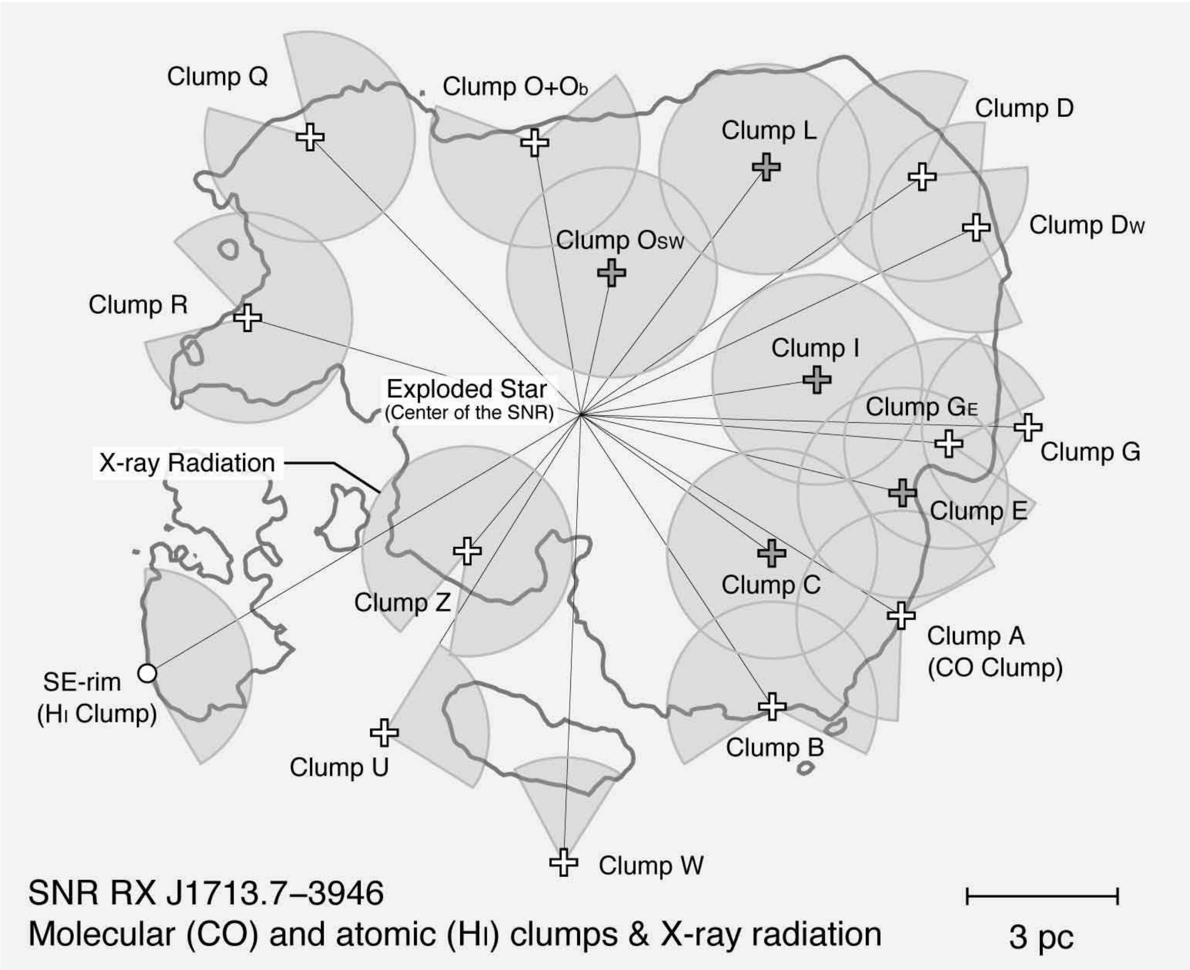


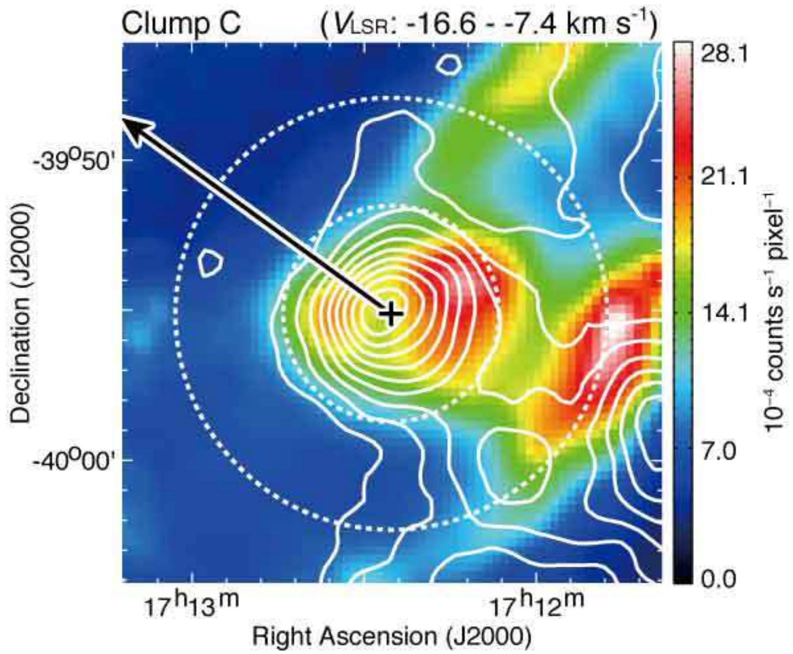


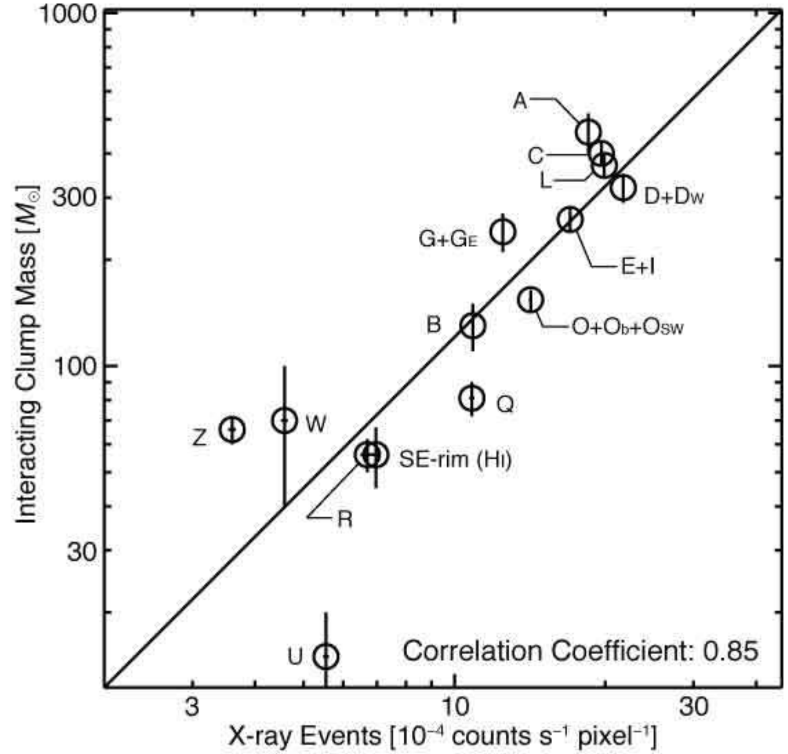

# MHD simulations of shock-cloud interaction

density vs. magnetic field

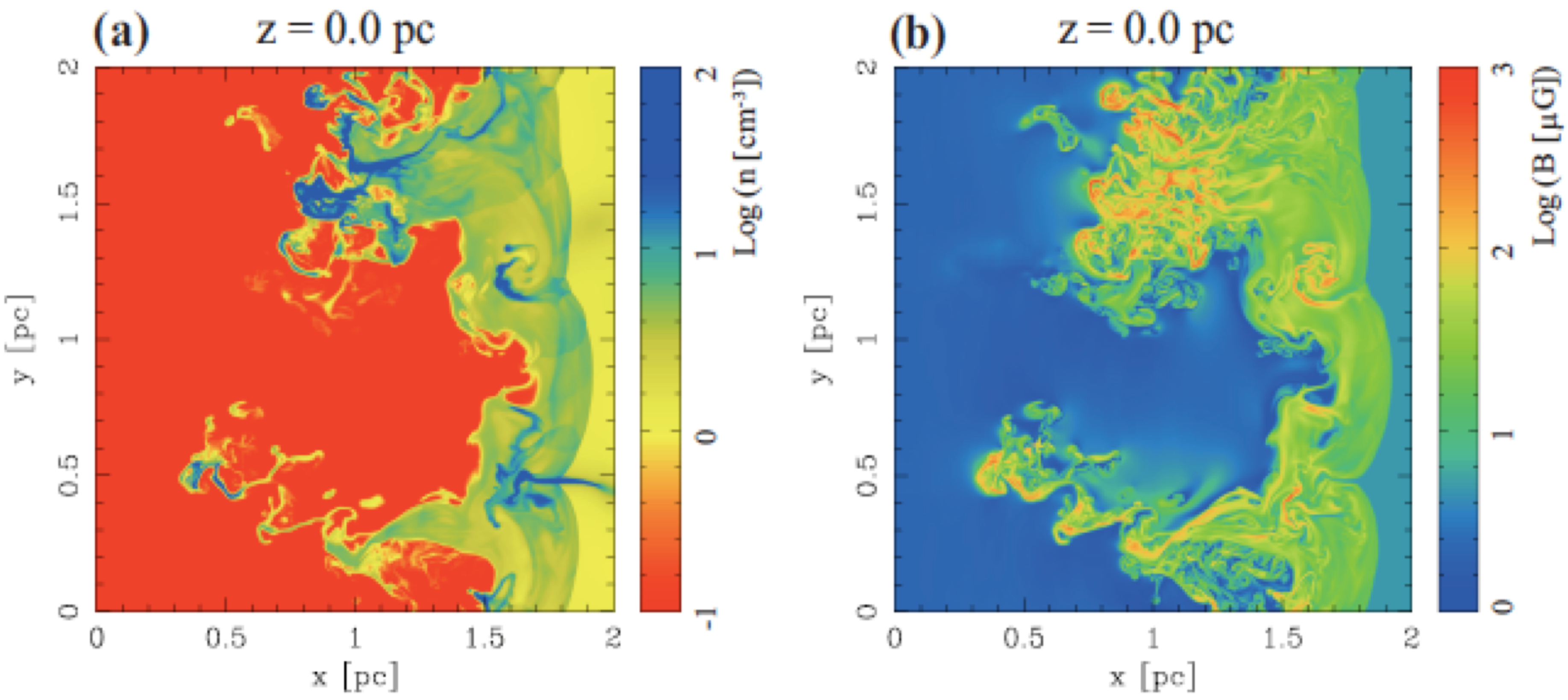


Inoue+ 2012

# MHD simulations of magnetic field vs. ISM density in RX J1713

Inoue+ 2012

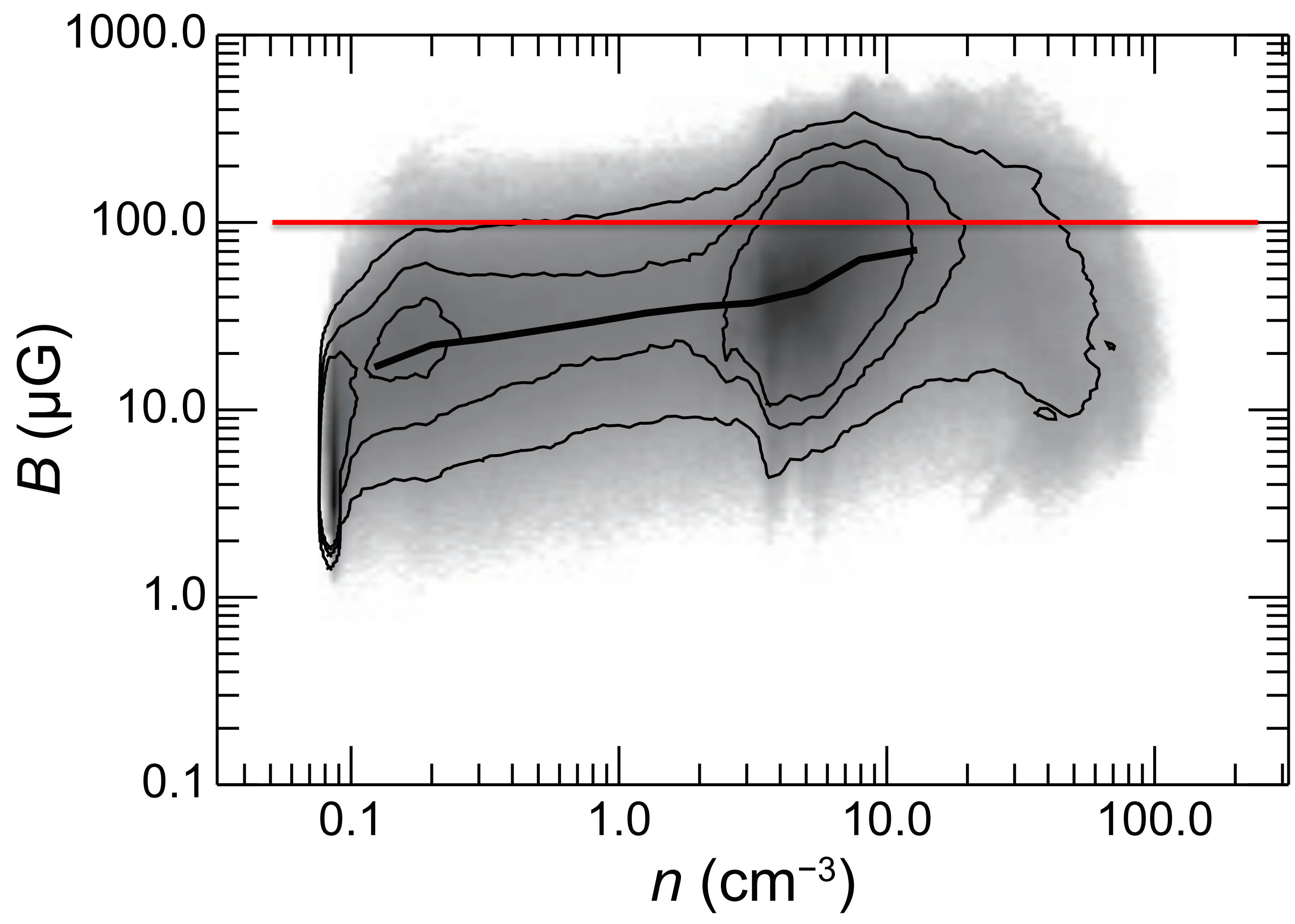

# Hadronic dominant broad band spectrum

## Zirakashvili & Aharonian 2010

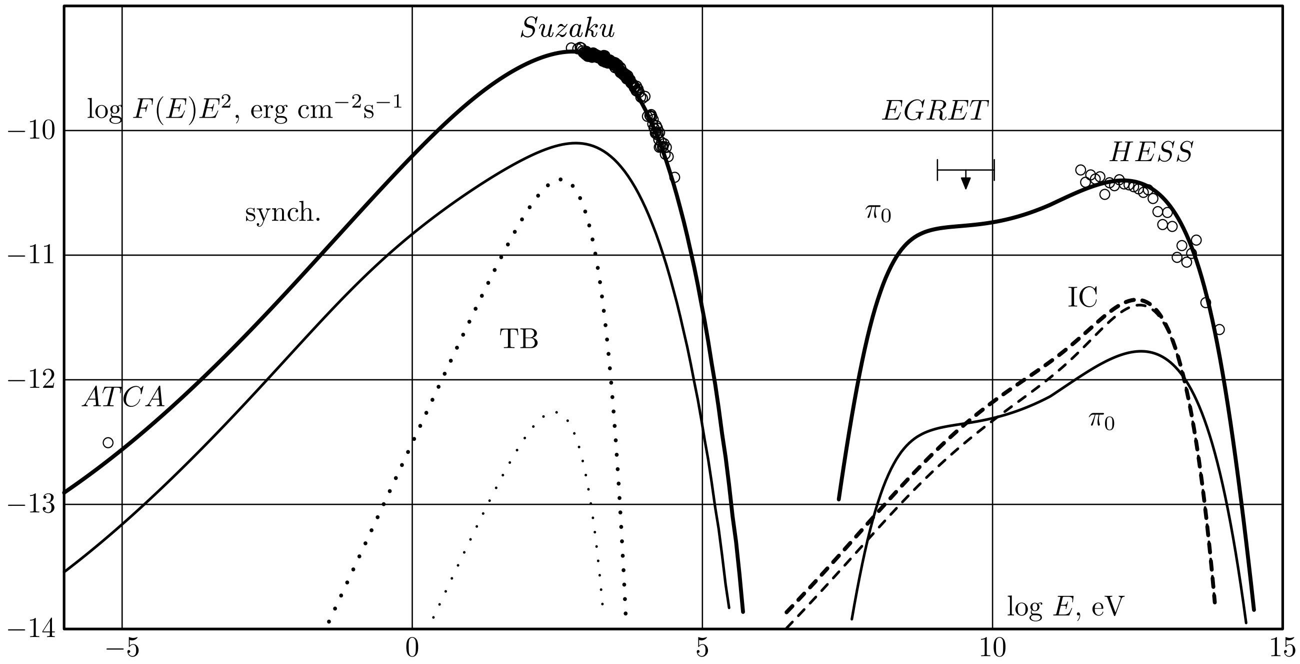


Fig. 6.— The results of modeling of of nonthermal radiation of RX J1713.7-3946 within the hadronic scenario of gamma-ray production. The following basic parameters are used: $t = 1620$ yr, $D = 1.2$ kpc, $n_H = 0.09$ cm$^{-3}$, $E_{SN} = 2.7 \cdot 10^{51}$ erg, $M_{ej} = 1.5M_{\odot}$, $M_A^f = M_A^b = 23$, $\xi_0 = 0.05$, the electron to proton ratios at the forward and reverse shocks $K_{ep}^f = 10^{-4}$ and $K_{ep}^b = 1.4 \cdot 10^{-3}$. The calculations lead to the following values of the magnetic fields and the shock speeds at the present epoch: the magnetic field downstream of the forward and reverse shocks $B_f = 127$ $\mu$G and $B_b = 21$ $\mu$G respectively, the speed of the forward shock $V_f = 2760$ km s$^{-1}$, the speed of the reverse shock $V_b = -1470$ km s$^{-1}$. The following radiation processes are taken into account: synchrotron radiation of accelerated electrons (solid curve on the left), IC emission (dashed line), gamma-ray emission from pion decay (solid line on the right), thermal bremsstrahlung (dotted line). The input of the reverse shock is shown by the corresponding thin lines. Experimental data in gamma-ray (HESS; Aharonian et al. 2007a) and X-ray bands (Suzaku; Tanaka et al. 2008), as well as the radio flux $22 \pm 2$ Jy at 1.4GHz (ATCA; Acero al. 2009) from the whole remnant are also shown.

# Hybrid origin broad band spectrum

## ZA10

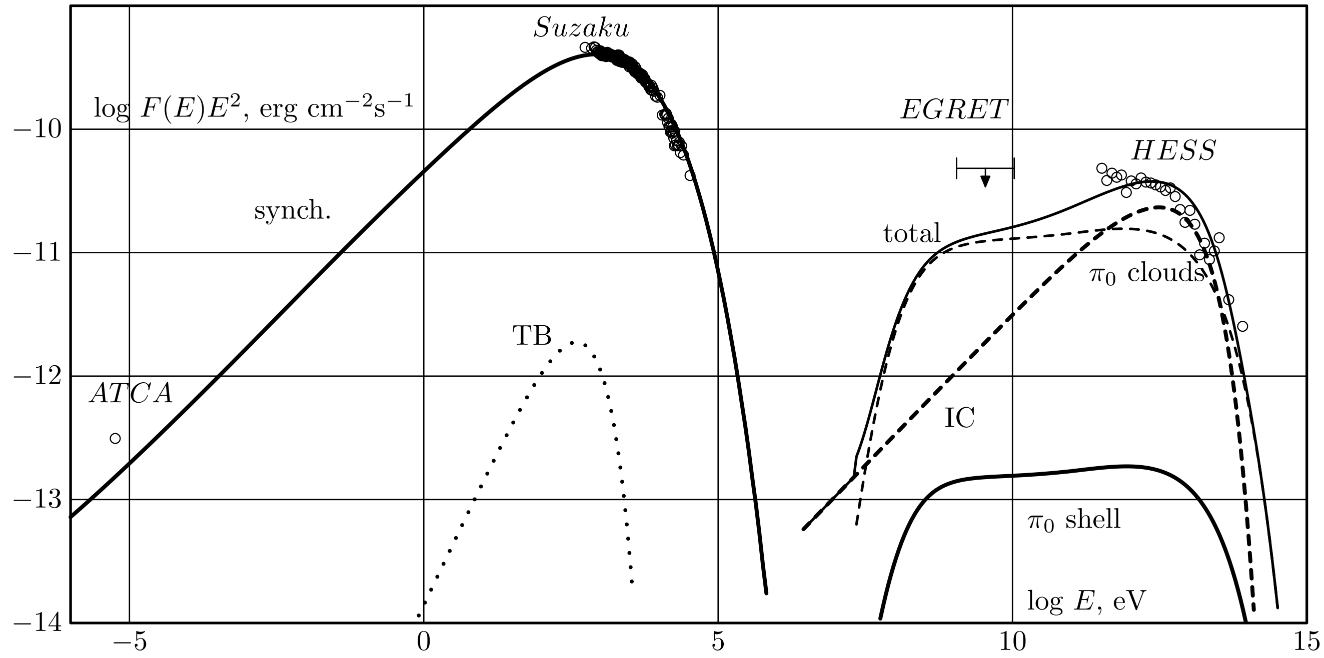


Fig. 14.— Broad-band emission of RX J1713.7-3946 for the composite scenario of gamma-rays with a non-modified forward shock and dense clouds. The principal model parameters are: $t = 1620$ yr, $D = 1.5$ kpc, $n_H$ =0.02 cm$^{-3}$, $E_{SN} = 1.2 \cdot 10^{51}$ erg, $M_{ej} = 0.74 M_\odot$, $M_A^f = 55$, $M_A^b = 10$, $\xi_0 = 0.1$, $K_{ep}^f = 1.4 \cdot 10^{-2}$, $K_{ep}^b = 9 \cdot 10^{-4}$. The calculations lead to the following values of the magnetic fields and the shock speeds at the present epoch: the magnetic field downstream of the forward and reverse shocks $B_f = 22\ \mu$G and $B_b = 31\ \mu$G, respectively, the speed of the forward shock $V_f = 3830$ km s$^{-1}$, the speed of the reverse shock $V_b = -1220$ km s$^{-1}$. The following radiation processes are taken into account: synchrotron radiation of accelerated electrons (solid curve on the left), thermal bremsstrahlung (dotted line), IC gamma-ray emission of the entire remnant including forward and reverse shocks (dashed line), hadronic component of gamma-rays from the remnant's shell (solid line on the right) as well as from dense clouds assuming the factor of 120 enhancement of the flux (thin dashed line). We also show the total gamma-ray emission from the entire remnant including the dense clouds (thin solid line).

# Gamma-ray spectrum of RXJ1713

Abdo+ 2011

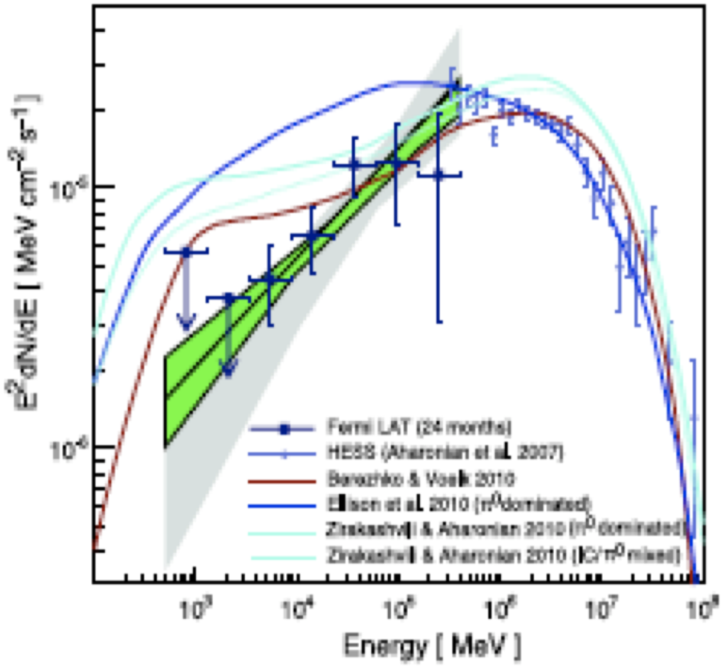


*S. Gabici and F. A. Aharonian*

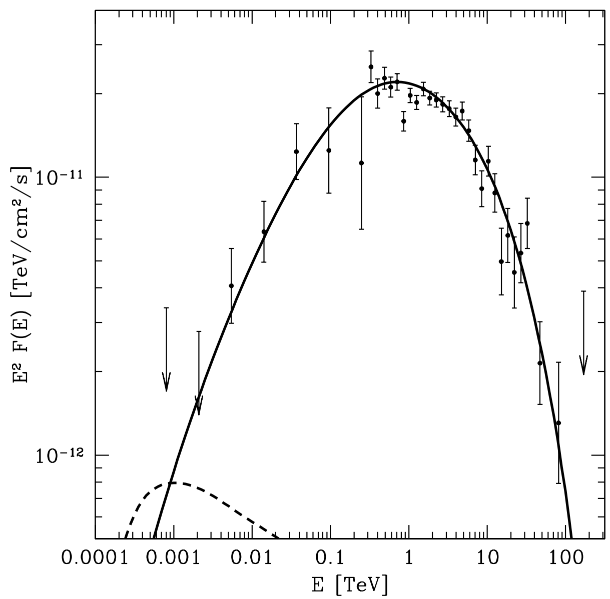


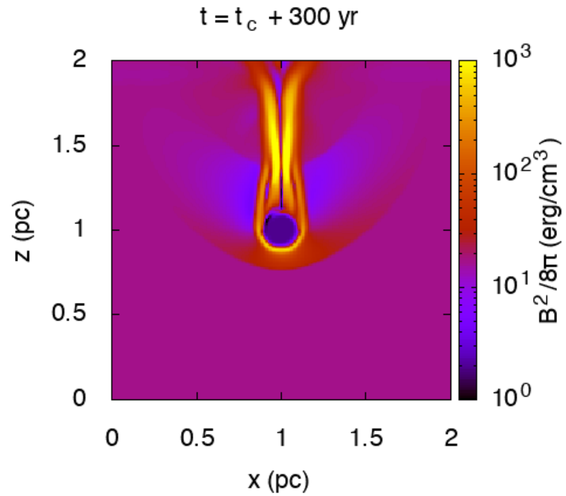


The hard spectrum is not unique to the leptonic scenario
The hard spectrum is explained by energy dependent penetration of CR protons into dense molecular gas.
(Inoue+ 2012, Gabici & Aharonian 2014, Celli+ 2018)

# Summary : Gamma rays are composite origin in RX J1713

Hadronic vs. leptonic

ー hadronic and leptonic components 70%:30% in RX J1713

first quantification of the two origins

ー Fukui+ 12; too low spatial resolution, three times coarser than the present data

ー the total CR energy is nearly the same with Fukui+ 12, SNRs are the main site of CR acceleration in the Galaxy

What is essential in hadronic gamma ray production

ー The large amount of the interstellar protons (10^4 Mo) causes the significant hadronic component.

ー The shell-like interstellar distribution was created by the stellar winds of the progenitor in Myr. RX J1713 is a core collapse SNR formed in the cloud.

ー Hadronic fraction of gamma rays depends on the ambient target proton mass. Only the interstellar proton mass, once association confirmed, may allow us to estimate the hadronic gamma rays even in unresolved sources.

# Future : Gamma rays are composite origin

Next steps

ー Second case, RX J0852 etc.

CTA will increase the number of spatially resolved SNRs

ー Improved statistics, probe spatial variation of the CR spectrum. More details of acceleration process

ー Neutrino detection; prediction will be made from the present hadronic gamma ray count

The interstellar proton mass is essential to quantify the hadronic process